EVALUATING SEPARATE IMPACTS OF LAND USE, LAND COVER AND CLIMATE CHANGE ON STREAMFLOW IN UPPER GIDABO WATERSHED, SOUTHERN ETHIOPIA

MSc THESIS

DEGEFU DOGISO BUKURE

HAWASSA UNIVERSITY, HAWASSA, ETHIOPIA

February, 2019

EVALUATING SEPARATE IMPACTS OF LAND USE, LAND COVER AND CLIMATE CHANGE ON STREAMFLOW IN UPPER GIDABO WATERSHED, SOUTHERN ETHIOPIA

DEGEFU DOGISO BUKURE

THE THESIS SUBMITTED TO THE HAWASSA UNIVERSITY SCHOOL OF GRADUATE STUDIES INPARTIAL FULFILLMENT OF THE REQUIREMENTS FOR THE DEGREE OF MASTER OF SCIENCE IN SOIL AND WATER CONSERVATION ENGINEERING

MAJOR ADVISOR: MIHRET DANANTO (PhD)

CO-ADVISOR: ALEMAYEHU MULUNEH (PhD)

HAWASSA UNIVERSITY INSTITUTE OF TECHNOLOGY, SCHOOL OF BIOSYSTEM AND ENVIRONMENTAL ENGINEERING

February, 2019

SCHOOL OF GRADUATE STUDIES

HAWASSA UNIVERSITY

ADVISORS' APPROVAL SHEET

This is to certify that the thesis entitled "**Evaluating Separate Impacts of LULC and Climate Change on Stream Flow in upper Gidabo Watershed**" submitted in partial fulfillment of the requirements for the degree of Master of "**Soil and Water Conservation Engineering**" the Graduate Program of the School of Biosystem and Environmental Engineering, and has been carried out by "**Degefu Dogiso Bukure**" ID.No. "SWCE-R/006/09" under our supervision. Therefore, we recommend that the student has fulfilled the requirements and hence hereby can submit the thesis to the school of Biosystem and Environmental Engineering.

______________________	______________________	______________________
Name of the major advisor	signature	date
______________________	______________________	______________________
Name of the co-advisor	signature	date

SCHOOL OF GRADUATE STUDIES

HAWASSA UNIVERSITY

EXAMINERS' APPROVAL SHEET

We, the undersigned, members of the Board of Examiners of the final open defense by **Degefu Dogiso Bukure** have read and evaluated his thesis entitled "**Evaluating Separate Impacts of LULC and Climate Change on Stream Flow in upper Gidabo Watershed**", and examined the candidate. This is, therefore, to certify that the thesis has been accepted in partial fulfillment of the requirements for the degree of Masters in "Soil and Water Conservation Engineering."

______________________	______________________	______________________
Name of the chairperson	signature	date
______________________	______________________	______________________
Name of the major advisor	signature	date
______________________	______________________	______________________
Name of the co-advisor	signature	date
______________________	______________________	______________________
Name of the internal examiner	signature	date
______________________	______________________	______________________
Name of the external examiner	signature	date
______________________	______________________	______________________
SGS approval	signature	date

Final approval and acceptance of the thesis is contingent upon the submission of the final copy of the thesis to the School of Graduate Studies (SGS) through the School Graduate Committee (DGC/SGC) of the candidate's department.

Stamp of SGS Date: _____________

ACKNOWLEDGEMENT

First of all, thanks to the Almighty God for granting me his limitless care, love and blessings all along the way. Next to that, my sincere gratitude goes to my research advisors, Dr. Mihret Dananto and Dr. Alemayehu Muluneh for their unreserved advice, guidance and constant encouragement. The careful comments I have received from them throughout my thesis work helped me to complete it successfully. It was their skillful contribution and constant encouragement that made me strong to face every up and down with confidence during the research study.

I am indeed grateful to my wife Meskerem Mulugeta for her persistent love, patience, support, continuous moral and encouragement during my graduate study. I wish if I could list all individuals who stood by my side, but I simply forward my heartfelt thanks and appreciation.

I am also thankful to the Ministry of Water, Irrigation and Energy of Ethiopia and the National Meteorological Agency of Ethiopia for providing me all the relevant data used as input for my research findings.

Finally, my heartfelt thanks to Aroresa Woreda Administration for their financial support and encouragement during my thesis works especially Aroressa Woreda Agricultural Office that directly or indirectly contributed to the success of the study.

DECLARATION OF THE FINAL THESIS

I hereby declare that all the corrections and recommendations suggested by the board of examiners are incorporated into the final thesis entitled "**Evaluating Separate Impacts of LULC and Climate Change on Stream Flow in Upper Gidabo Watershed**" by Degefu Dogiso Bukure.

Name of the designate	Signature	date

LIST OF ACRONYMS

95PPU	95 Percent Prediction Uncertainties
AGL	Agricultural Land
BULT	Built-up Area
CFSR	Climate Forecast System Reanalysis
DEM	Digital Elevation Model
ERDAS	Earth Resource Data Analysis System
EROS	Earth Resources Observation System
ETM+	Enhanced Thematic Mapper Plus
FAO	Food and Agricultural Organization
FOREV	Evergreen Forest
FORMX	Mixed Forest
GCM	Global Climate Model
GIS	Geographical Information Science
GPS	Global Positioning System
GRL	Grazing Land
HRU	Hydrological Response Unit
IHDM	Institute of Hydrology Distributed Model
IPCC	Intergovernmental Panel on Climate Change
LULCC	Land Use and Land Cover Change
MWIE	Ministry of Water, Irrigation and Energy
NMA	National Metrological Agency
NSE	Nash-Sutcliffe Efficiency
OFAT	One Factor at a Time
OLI	Operational Land Imager
PBIAS	Percent Bias
Q_{surf}	Surface Runoff
Q_{lat}	Lateral Flow
Q_{base}	Base Flow
RMSE	Root Mean Square
SCS	Soil Conservation Service

SDSM	Statistical Downscaling Model
SHE	Systéme Hydrologique Européen
SIMHYD	Simplified Hydrology Model
SNNPRS	Southern Nation Nationality and People Regional State
SPSS	Statistical Program for Social Science
SRTM	Shuttle Radar Topographic Mission
SUFI-2	Sequential Uncertainty Fitting Version 2
SWAT	Soil and Water Assessment Tool
SWAT-CUP	SWAT Calibration and Uncertainty Programs
TIRS	Thermal Infrared Sensor
TM	Thematic Mapper
TOPMODEL	Topography Based Hydrologic Model
USGS	United States Geological Survey
UTM	Universal Transverse Mercator
VIC	Variable Infiltration Capacity
WGS	World Geodetic System

LIST OF TABLES

LIST OF FIGURES

LIST OF APPENDICES

TABLE OF CONTENTS

ABSTRACT

LULC and climate change are two factors that produce major impacts on stream flow and separation of these impacts is important for water resources management as well as policy adaptation and planning for sustainable watershed development. This study was mainly focused on separating the combined and isolated impacts of LULC and climate change on stream flow reduction in upper Gidabo watershed, Southern Ethiopia. The hydrological modeling with the one factor at a time (OFAT) analysis was employed to separate hydrological impacts of LULCC from those of climate change. The SWAT model and MK statistics test were used for the study. SWAT was calibrated and validated in the watershed. The results confirmed that SWAT was a powerful and accurate model for the watershed. The model assessment metrics: NSE, R^2 and PBIAS in the data were 0.90, 0.91 and 5% respectively for the calibration period and 0.73, 0.75 and 12.4% respectively for the validation period. After the calibration and validation of the SWAT model, four different scenarios were developed based on one factor at a time (OFAT) experiment. By comparing, the simulated mean annual stream flow components (Q_{surf}, Q_{lat} and Q_{base}) results of S1 vs. S2, S3 and S4 for evaluating the effect of LULC and climate change and both on stream flow. The assessment of MK statistics result of climate change showed that precipitation and stream flow exhibited a downward trend and air temperature exhibited upward trends significantly from 1985 to 2016. Evaluation of LULCC from 1985 to 2016 showed that the changes in growth of agricultural land and built-up areas have increased by the annual rate of change 1.81% and 2.33% respectively whereas the mixed forest, evergreen forest and grassland has reduced by the rate of change 1.27%,1.84% and 0.30% respectively. The combined effects of LULC and climate change reduced mean annual lateral flow and base flow values by 7.17mm/yr. and 94.74mm/yr. respectively. The LULCC increased surface runoff by 38.29mm/yr. (56.5%) decreased lateral flow and base flow by 6.23mm/yr. (86.89%) and 26.48mm/yr. (27.95%) respectively while climate change decreased surface runoff, lateral flow and base flow by 29.47mm/yr. (43.5%),0.94mm/yr. (13.11%) and 68.26mm/yr. (72.05%) respectively. Generally, the climate change had the higher impact on base flow reduction while LULCC had higher impact on surface runoff increment and lateral flow reduction in the study watershed. Therefore, to mitigate the negative impacts of climate change combined with LULC change, local and national policymakers are encouraged to apply science-based watershed and land use planning and implement appropriate management approaches in the upper Gidabo watershed.

Key words: LULCC, Climate change, SWAT, Stream flow, upper Gidabo watershed

CHAPTER ONE

1. INTRODUCTION

1.1. Background of the Study

Developing countries like Ethiopia where agriculture serves as the backbone of the economy and ensure the wellbeing of the people, the adverse effects of land use and land cover changes are diverse. On the other hand, many of the world's countries already struggle under existing water stress from pressures such as irrigation demands, industrial pollution, and water-borne sewerage. These pressures will be significantly exacerbated by climate change, which for many regions will result in reduced rainfall and increasing temperatures further reducing the availability of water for drinking, household use, agriculture and industry (Melese, 2016).

Land use and cover change can affect hydrological processes such as evapotranspiration, interception, infiltration and surface runoff by directly altering morphological and physiological conditions of the landscape and by indirectly modifying soil and atmospheric boundary layers (Cuo, 2016). Meanwhile, climate change particularly the shifts in precipitation and temperature can also exert a profound impact on hydrological conditions and spatial-temporal patterns of water resources (Sorribas *et al*., 2016; Sunde *et al*., 2017).

Manish and Rawat (2015) concluded that expansion of agriculture, urbanization, deforestation and the day to day activities of mankind resulted to temporal and spatial change in land use and land cover that have affected water flow pathways and water balance.

Different recent studies show that LULC and climate change are two of the most significant drivers of hydrological variations (Kundu *et al*., 2017; Trang *et al*., 2017). As a result, the impact assessments of LULC and climate change have got considerable attention from the scientific community as well as decision and policy makers in the context of increasing water scarcity (Wagner *et al*., 2017; Gao *et al*., 2016). LULC and climate change generally intertwine together in their impacts on hydrological regimes (Zhang *et al*., 2016).

The study conducted by Melese (2016) concluded that the climatic impact on the water regime might also make worse other environmental and social effects of water management. For instance, reduced river runoff can concentrate the effects of pollutants or exacerbate the spread of water-borne disease. Climate fluctuations can also affect the use of agricultural land associated with irrigation systems.

In upper Gidabo watershed, the land and water resources of the watershed are in danger due to the rapid growth of population, deforestation, overgrazing, soil erosion, soil storage capacity reduction, drainage, water logging, and the shortage of rain and water pollution. Thus, to improve the watershed management programs; the impact assessment research of climate change, land use and land cover change on stream flow is needed.

In River Basin management, watershed hydrological models have a vital role in simulating possible feature changes and their impacts. This helps to determine improved measures of river basin management (Valentina *et al*., 2014). Understanding the hydrological processes is crucial towards the better water and land resource management as the hydrology largely influences soil erosion and is highly important to agricultural productivity (Easton *et al*., 2010).

There are various rainfall-runoff models developed for accounting of hydrological processes. They are classified as physical, empirical and conceptual models. The soil and water assessment tool (SWAT) model was developed to evaluate the impact of climate and land management practices on the water in large and complex watersheds with varying land use, soils and management conditions over long periods of time (Arnold *et al*., 1998). Various researchers have evaluated the SWAT model, and their findings indicated that SWAT is capable of simulating hydrological processes with reasonable accuracy and can be applied to all types of gauged basins. Therefore, to determine the impact assessment of LULCC and climate change on the stream flow of the watershed, SWAT- 2012 model with Arc GIS 10.3.1 interface was selected for the present study.

1.2. Statement of the Problem

Although Ethiopia is also known as a tower of East Africa, today many rivers and lakes become shrinking in size due to the decrease in river flow and some small streams dry up completely and finally the magnitude of flow of the medium to large rivers will decrease significantly (Melese, 2016).

In the Gidabo watershed, multitudes of economic activities are being carried out along the major as well as small stream courses. At the lower course of the rivers, a number of agro processing industries are now coming into the river courses. Many new settlements both in urban and rural are coming into being and the existing ones are growing in population size at alarming rates. The watershed is also facing continuous land use and land cover change that has impacted the water balance of the watershed by changing the magnitude and pattern of the components of stream flow which are the surface runoff, lateral flow, and base flow that result increasing the extent of the water management problems (Zewude,2016).

The other problems of the watershed are; the annual rainfall is decreasing significantly, the temperature is increasing and stream flow is generally decreasing. The findings of Belihu *et al*. (2018) in Gidabo River Catchment revealed that the annual rainfall trends exhibited a significant decrease by about 12 mm per year in the upstream, which is largely driven by the significant decrease in the peak season rainfall. The temperature analyses also revealed that the catchment was getting warmer particularly in the upstream. The minimum temperature trend showed a significant increase of about 0.08°c per annum. There is generally a decreasing trend in stream flow.

The Groundwater recharge is also decreasing due to climate change. According to the study conducted by Mechal *et al*. (2015) in Gidabo River Basin revealed that the long-term average recharge estimated by SWAT model shows a strong spatial variability and reveals a remarkable decrease from the highland towards the rift floor reflecting the large differences in climatic conditions as well as soil and land use characteristics. The average annual recharge for 1998-2010 reveals a remarkable decrease from the highland (410 mm/year) towards the rift floor (25 mm/year). Both the spatial and temporal recharge variability is mainly controlled by the climate change.

According to the study by Shanka (2017), Climate change meaningfully affects the runoff, flooding and the river flow in Gidabo River Catchment by showing significant variation in the monthly, seasonal and annual runoff.

In general, previous studies in the entire Gidabo River Basin mainly focus on three issues; past land use changes and their impacts on stream flow, past climate changes and their impacts on stream flow. In the study watershed stream flow is decreasing, according to the studies this reduction originated from LULCC and climate change. There are obviously some deficiencies in the studies. The studies were not studied by combining both factors (LULC and climate change) and did not identify the quantity of their isolated and combined effects on stream flow reduction. The studies also did not identify which factor has dominant impact (either climate change or LULCC) on stream flow reduction. Thus, this study examined isolated and combined impacts of LULC and climate change on the stream flow reduction in the upper Gidabo watershed by using a semi-distributed hydrologic model, SWAT.

1.3. Objectives of the Study

1.3.1. General objective

To identify combined and isolated impacts of LULC and climate change on stream flow reduction in the upper Gidabo watershed by using hydrological modeling approach.

1.3.2. Specific objectives

i. To examine the trends in LULCC in different years (1985, 2002 and 2016) in the upper Gidabo watershed.
ii. To assess the trends in mean annual temperature and annual rainfall.
iii. To investigate the impacts of LULCC and climate change on stream flow reduction in the upper Gidabo watershed.
iv. To avail the compared effects of LULC and climate change on stream flow reduction in the upper Gidabo watershed.

1.4. Research Questions

i. What was the contribution of climate change and LULCC to stream flow reduction in the past, from 1985 to 2016 in the watershed?
ii. Which is the major driving factor (climate or LULCC) for stream flow reduction in the watershed?
iii. What was the historical, mean annual trend of temperature and rainfall?
iv. What was LULCC trend in the study watershed?

1.5. The Significance of the Study

This study provides awareness into stream flow responses to the combined climate and land use changes in upper Gidabo watershed in the past. Understanding how land use and climate changes affect stream flow in the watershed, which would help watershed managers, agricultural producers, policymakers. Moreover, it may help in the development of adaptive measures in response to climate change; and may reduce unnecessary losses from the water cycle. It will help with the provision of a reliable water source for food production and human consumption; and development of sustainable water management strategies that will enable the desired level of functionality within the local ecosystem.

1.6. Organization of the Thesis

The paper was organized into five sections: Section one is an introduction section where the background, statement of the problem, objectives of the study, research questions and significance of the study were discussed. In section two, review of related literature where the definition and concepts of land use and land cover changes, climate change, application of hydrological models, an introduction to SWAT model, application of SWAT model worldwide, in Ethiopia and Gidabo River Basin were reviewed. Data and methodology section in which description of the study area, image processing, classification and accuracy assessment, hydrological model selection criteria, collection of input data and analysis, model setup, model performance evaluation and evaluation of stream flow due to land use and land cover changes and climate change were elaborated in section three. The fourth section describes the result and discussion which are land use and land cover analysis, stream flow modeling and evaluation of stream flow due to land use and land cover change and climate change. The land use and land cover analysis including land cover maps and statistics, and accuracy assessment. The stream flow modeling includes parameter sensitivity analysis, calibration and validation, and the performance evaluation of the model. Finally, in section five, the conclusions and recommendations of the study were provided.

CHAPTER TWO

2. LITERATURE REVIEW

2.1. Land Use and Land Cover Change: Definitions and Concepts

Land use: - is the human modification of natural environment or wilderness into a built environment. It is basically the human activities on the earth's surface. Land cover, on the other hand, is simply that which covers the earth surface (Musa and Odera, 2015).

Land cover change: - refers to complete or partial replacement of one cover type by another. **Land use change: -** includes the modification of land cover types such as intensification of agricultural use without changing its overall classification (Veldkamp, 2001).

Land use and land cover change: - is commonly grouped into two broad categories: conversion and modification (Meyer and Turner, 1994). Conversion refers to a change from one cover or use category to another (e.g. from forest to grassland). Modification, on the other hand, represents, a change within one land use and land cover category (e.g. from rain-fed cultivated area to irrigated cultivated area) due to changes in its physical or functional attributes.

2.1.1. Impacts of land use change on hydrology

Land use and land cover (LULC) changes influence hydrological processes by altering interception rates, soil water, evapotranspiration, infiltration and groundwater leading to changes in surface runoff, stream flow and flood frequency (Wu *et al*.,2013; Zhang *et al*., 2014).

Evapotranspiration and soil moisture

LULCC plays an important role in influencing the water cycle through changes in evapotranspiration, soil water holding capacity and the vegetation's ability to intercept precipitation (Zhang *et al*., 2014). Evapotranspiration is one of the most significant components of the hydrologic budget, which is a combination of two sub-processes: evaporation and transpiration. Evaporation is water loss from open water bodies, wetlands, bare soil, snow cover, etc. while transpiration is water loss from living plant surfaces. Thus, land surface characteristics influence the process of evapotranspiration (Hanson, 1988).

Surface runoff and groundwater

LULC changes alter vegetation cover and surface roughness that affect the timing and magnitude of surface runoff and groundwater discharge, leading to changes in stream flow and magnitude and frequency of floods (Schilling *et al*., 2014). Land use changes, such as urbanization and agricultural activities cause greater surface runoff (Pai and Saraswat, 2011).

Deforestation may also cause greater surface runoff. In East Africa, Baker and Miller (2013) reported that due to land conversion from forest to agricultural land increased surface runoff. Ghaffari *et al*. (2010) showed that decreasing grassland and increasing agricultural land decreased groundwater recharge and base flow in the semi-arid Zanjanrood Basin in Iran.

Stream flow and flood

Increasing land use conversion (especially for urbanization, deforestation, grassland depletion) can potentially lead to an increase in stream flow and flood frequency (Schilling *et al*., 2014). During storm events, greater surface runoff can exceed the flow carrying capacity of the stream within the watershed, which may increase the risk of potential flooding. In addition, grassland expansion can reduce flood potential due to a decrease in stream flow. Grassland has higher evapotranspiration compared to agricultural land and may promote higher infiltration, leading to a reduction of flood potential in the watershed.

2.2. Climate Change

Climate change is a long-term continuous change (increase or decrease) to average weather conditions (e.g. average temperature) or the range of weather (e.g. more frequent and severe extreme storms). Climate change is slow and gradual, and unlike year to year variability, is very difficult to perceive without scientific records. Climate change occurs because of changes to Earth's environment, like changes in its orbit around the sun or human modification of the atmosphere (US global change, 2009).

It should be noted that climate evolution in recent decades is a combination of human-induced climate change (e.g. increased greenhouse gas emissions) and naturally induced climate change caused by internal forcing. Hydrologists tend to use the terminology ‘climate change' to reflect both human induced climate change and naturally induced climate change, and then quantify the effects on hydrological processes.

2.2.1. Impacts of climate change on hydrology

Climate change is perceived to have been driven by global warming, in turn, is resulting in the changes in the temporal and spatial distribution of precipitation patterns (IPCC, 2014). Global climate change is one major factor that directly affects hydrological processes (Zhang *et al.*, 2016) and global warming is identified as an important issue regarding climate change during the coming century (Chien *et al*., 2013).

Potential impacts of changes in climate (e.g. precipitation and temperature) may cause variations in hydrological processes including evapotranspiration, surface runoff, timing and magnitude of stream flow, and flood events (Kumar and Neupane, 2015). Temperature variation and wind speed affect evaporation and transpiration sub-processes, which influence surface and sub-surface water budgets (Hu *et al.*, 2015).

Evapotranspiration

Evaporation is the sub-process of evapotranspiration, which varies by season of the year, time of the day and availability of soil water. Evaporation rate is influenced by solar radiation, air temperature, humidity and wind speed (Hanson, 1988). Solar radiation and air temperature provide the energy to evaporate the water from open water bodies such as a lake, reservoir and stream, while the air humidity and wind speed control evaporation processes.

Another sub-process the transpiration depends on the water availability in the soils and plants. The plant root takes water and transfers it into the atmosphere. Consequently, temperature and precipitation increases result in increased evapotranspiration (Zhang *et al*., 2016). For example, Guo *et al*. (2008) reported that during dry seasons, lower temperature and higher humidity resulted in decreased evapotranspiration in the Poyang Lake Basin in China.

Ficklin *et al*. (2013) noticed that in California, projected increased temperature and decreased precipitation might result in an increase in evapotranspiration. The researchers noticed that seasonal trends in evapotranspiration also follow seasonal trends in solar radiation and air temperature. In China, due to potential higher temperature and increased precipitation, increased trends in evapotranspiration were observed in the wet season (June to September) (Zhang *et al*., 2016).

Surface runoff

Precipitation is the source of water in the watershed and the available water is minus water by evapotranspiration.

Available water contributes to surface runoff and stream flow (Kanae and Oki, 2006). Therefore, increased precipitation may lead to an increase in surface runoff while a decrease in precipitation can result in the opposite effects (Jianyun and Lirong, 2012).

Stream flow and flood

Many studies have revealed that climate change is expected to accelerate the global hydrological cycles and affect stream flow (Driessen *et al*., 2010; Ficklin *et al*., 2013; Jha and Gassman, 2014). These studies revealed that stream flow variability is closely related to climate changes.

Studies showed that due to climate change, precipitation would increase on average, while globally evapotranspiration may not increase as much as precipitation because elevated CO_2 concentration may induce stomata closure and reduce transpiration (Kanae and Oki, 2006). Climate change studies by potential climate variability may increase flood risk around the world.

2.2.2. General implications of changing climate on hydrology

Changes in the earth's climate can have multiple significant implications for hydrologic regimes. Increased concentrations of greenhouse gas will cause much of the solar radiation to be trapped inside the earth, hence elevating its temperature (Trenberth, 1998). Rising global temperatures will lead to changes in the characteristics of the hydrologic cycle influencing the spatiotemporal characteristics of precipitation and rainfall, runoff, and potential evapotranspiration (IPCC, 2007). For example, the intensification of the hydrologic cycle that has been observed can lead to a decrease in precipitation in sub-tropical areas, which then increases the probability of drought (Dai *et al*., 1998; Huntington, 2006).

On the other hand, increased annual precipitation in the tropics and at high latitudes will lead to an increasing probability of floods (Huntington, 2006). The melting of glaciers and rising sea levels because of climate change can threaten freshwater supplies (Jackson *et al*., 2001). These overall changes are likely to have a strong influence on the environment, including water resources availability and accessibility, and therefore pose challenges in water resources planning and management.

2.2.3. Trend detection and analysis in hydro-climatic variables

Trend analysis in hydro-climatic variables is one way to assess how the climate has changed over time. Trend detection refers to methods used to extract an underlying behavioral pattern in a time series otherwise that would be partly or fully hidden by noise. The detection of abrupt and gradual changes in hydrological and meteorological records has been explored in considerable detail by researchers.

Information about spatio-temporal variability in hydro-climatic time series is of great importance from both scientific and practical viewpoints. For example, the interpretation of the significance of trends existing in the annual maximum (flood), mean, and low flows in rivers is very valuable for flow regulation (Tharme, 2003). This is because they are considered when designing flood mitigation structures, flood protection systems, and water storage reservoirs.

Trend detection and forecasting of low flow are of importance due to the quantity of water to be released downstream of a dam, in order to protect ecological integrity and sustainability (Smakhtin, 2001).

2.2.4. Application of Mann-Kendall statistics test for climate trend analysis

According to the study by Anzhou *et al*. (2016) in the Weihe River Basin of northwest China, concluded that, during 1980-2000, the farmland in the Weihe River Basin decreased by 1.4%, and the woodland, grassland and construction land increased by 0.6%, 0.2%, and 0.6%, respectively, due to land use change. The Mann-Kendall test indicates a statistically insignificant decreasing trend in rainfall, but a statistically significant decreasing trend in temperature.

The study by Belihu *et al*. (2018) in Gidabo River Catchment; to detect climatic trends the analysis was done by using Mann-Kendal (MK), Sen's graphical method and to detect change point using the Pettit test. The comparison of trend analysis between MK trend test and Sen graphical method results showed the most similar pattern. The annual rainfall trends exhibited a significant decrease by about 12 mm per year in the upstream, which is largely driven by the significant decrease in the peak season rainfall. The Pettit test revealed that the years 1997 and 2007 were the change points.

The study by Belete (2013) in Lake Hawassa, by using the Mann-Kendall test Results of the Mann-Kendall trend analyses revealed the significant increasing trend of the lake level and stream flow. On the contrary, a decreasing trend of evaporation was observed while rainfall exhibits no trend over the study period.

2.3. Hydrologic Models

The purpose of a model is to represent a complex system in a simplified way. There is a wide variety of models to represent the complex hydrologic dynamics of the earth system. Various hydrologic models can be classified into categories as:

Lumped hydrologic models: - Lumped models assume the complete basin as a homogenous system without considering the spatial distribution of processes (Xu, 2002).

Semi-distributed hydrologic models: - These types of models calculate flow contribution from separate sub-basins, considering that the sub-basins are homogenous (Xu, 2002). Examples of semi-distributed hydrologic models are the TOPMODEL and Soil and Water Assessment Tool (SWAT) (Arnold *et al*., 2012; Neitsch *et al*., 2011).

Distributed hydrologic models: - In distributed models, the whole basin is divided into elementary units (i.e. areas are divided as a grid net where water flows from one grid point to another when water drains through the Basin) (Xu, 2002). Examples of distributed hydrologic models are the SHE and the Institute of Hydrology Distributed Model (IHDM).

2.3.1. The SWAT model

The Soil and Water Assessment Tool (SWAT) is a semi-distributed, continuous time step, process-based river basin model (Arnold *et al*., 2012). SWAT has been widely used to analyze hydrological processes at watershed scales. The hydrological component of the model is based on a water balance equation with processes that include precipitation, surface runoff, water yield, evapotranspiration, lateral flow, percolation and groundwater flow (Arnold *et al*., 1998).

The model is computationally efficient. Simulation of a very large basin or a variety of management strategies can be performed without excessive investment of time and money. The model enables the users to study long-term impacts. Many of the problems currently addressed by users involve the gradual buildup of pollutants and the impact on downstream water bodies. To study these types of problems, results are needed from runs with output spanning several decades. SWAT is a continuous time model, i.e. a long-term yield model. The model is not designed to simulate detailed, single even flood routing (Neitsch *et al*., 2011).

No matter what type of problem studied with SWAT, water balance is the driving force behind everything that happens in the watershed. To predict accurately, the movement of pesticides, sediments or nutrients the hydrologic cycle as simulated by the model must conform to what is happening in the watershed can be separated into two major divisions: Land phase of the hydrologic cycle and water or routing phase of the hydrologic cycle. The land phase of the hydrologic cycle controls the amount of water, sediment, nutrient and pesticide loadings to the main channel in each sub-basin. The water phase of the hydrologic cycle can be defined as the movement of water and sediments etc. through the channel network of the watershed to the outlet (Neitsch *et al*., 2011).

The reasons behind for selecting the SWAT model for this study are; the model was applied for land use, land cover and climate change impact assessment on stream flow in different parts of the world (Setyorini *et al*., 2017; Yang *et al*., 2017; Yin *et al*., 2017; Zhang *et al*., 2017). The model simulates the major hydrological process in the watersheds. It is capable of yearly, monthly, daily or sub-daily simulation over long periods; it is ready and freely available. It combines studies of water quantity (river discharge, surface flow, lateral flow, base flow, drains, irrigation, reservoirs, and lakes).

SWAT is a relatively recent model used to assess the watershed hydrology (Jha, 2011). According to Kannan *et al*. (2007), it is the best among the different hydrological models due to its capability for application to large-scale watersheds (>100km^2), interface with a Geographic Information Science (GIS), continuous time simulations performance and generation of the maximum number of sub-basins and ability to characterize the watershed in enough spatial detail.

The SWAT model was developed to evaluate the impact of climate and land management practices on the water in large and complex watersheds with varying soils, land use and management conditions over long periods of time (Arnold *et al*., 1998). The SWAT model is a catchment scale hydrological model based on the principles of the water balance equation:

$$SW_t = SW_O + \sum_{i=0}^{t}(R_{day} - Q_{surf} - E_a - W_{seep} - Q_{gw} \qquad (2.1)$$

Where, $SW_t$is the final soil water content (mm),SW_0 is the initial soil water content on day i (mm), $t$is the time (days),$R_{day}$is the daily precipitation on a day i(mm),$Q_{surf}$is the amount of surface runoff on a day i(mm), $E_a$is the evapotranspiration on a day i(mm), W_{seep} is the amount of water entering the unsaturated zone on a day i(mm) and consists of the infiltration rate minus the capillary rise, and Q_{gw} is the amount of return flow on a day i(mm).

2.3.2. Components of stream flow

Surface runoff

Surface runoff refers to the portion of rainwater that is not lost to interception, infiltration, and evapotranspiration (Solomon, 2005). Surface runoff occurs whenever the rate of precipitation exceeds the rate of infiltration. SWAT offers two methods for estimating the surface runoff: The Soil Conservation Service (SCS) curve number method and the Green and Ampt infiltration method. The Green and Ampt method needs sub-daily time step rainfall, which made it difficult to be used for this study due to unavailability of sub-daily rainfall data. Therefore, the SCS curve number method was adopted for this study.

The general equation for the SCS curve number method is:

$$Q_{surf} = \frac{(R_{day} - I_a)^2}{(R_{day} - I_a + S)} \quad (2.2)$$

Where, Q_{surf} is the accumulated runoff or rainfall excess (mm), R_{day} is the rainfall depth for the day (mmH_2O), I_a is initial abstraction which includes surface storage, interception and infiltration prior to runoff (mmH_2O) and S is retention parameter (mmH_2O).

The retention parameter varies spatially due to changes in land surface features such as soils, land use, slope and management practices. These parameters also can be affected temporally due to changes in soil water content. It is mathematically expressed as:

$$\mathrm{S} = 25.4\left(\frac{1000}{\mathrm{CN}} - 10\right) \quad (2.3)$$

Where, CN is the curve number for the day and its value is the function of land use practice, soil permeability and soil hydrologic group.

The initial abstractionI_a, is commonly approximated as $0.2S$ and equation 2.2 becomes:

$$\mathrm{Q_{surf}} = \frac{(R_{day} - 0.2S)^2}{(\mathrm{R}_{day} - 0.8\mathrm{S})} \quad (2.4)$$

Runoff will only occur when $R_{day} > I_a$

Lateral flow/Interflow

Once the surface runoff is calculated from rainfall, the remaining amount of water is allowed to infiltrate in soil layers. The infiltrated water is then routed through soil layers by the storage routing methodology (Han *et al*., 2012; Neitsch *et al*., 2011). The storage routing method first fulfils the field capacity requirement of the upper soil layer and calculates if there is excess soil water available:

If there is excess soil water available, then the lateral flow from an HRU is calculated as:

$$Q_{lat} = 0.024\left(\frac{2 * SW_{ly.excess} * K_{sat.ly} * slp}{\emptyset_d * L_{hill}}\right) \quad (2.5)$$

Where, $K_{sat.ly}$ is saturated hydraulic conductivity (mm/hr.), slp is the steepness of a slope (m/m), $\emptyset_d$ is the drainable porosity of soil layer(mm/mm), $SW_{ly.excess}$ is the water content in a soil layer above the field capacity (mm), and L_{hill} is the hill slope length(m).

Base flow/Return flow

To simulate the groundwater SWAT partitions groundwater into two aquifer systems: a shallow, unconfined aquifer which contributes return flow to streams within the watershed and deep, confined aquifer which contributes return flow to streams outside the watershed (Neitsch *et al*., 2011). In SWAT the water balance for a shallow aquifer is:

$$aq_{sh,i} = aq_{sh,i-1} + W_{rchg} - Q_{gw} - W_{revap} - W_{deep} - W_{pump,sh} \quad (2.6)$$

Where, $aq_{sh,i}$ is the amount of water stored in the shallow aquifer on day i (mm), $aq_{sh,i-1}$ is the amount of water stored in the shallow aquifer on day $i-1$ (mm), W_{rchg} is the amount of recharge entering the aquifer on day i(mm), Q_{gw} is the groundwater flow, or base flow, or return flow, into the main channel on day i (mm), W_{revap} is the amount of water moving into the soil zone in response to water deficiencies on day i (mm), W_{deep} is the amount of water percolating from the shallow aquifer into the deep aquifer on day i (mm), and $W_{pump,sh}$ is the amount of water that is removed from the shallow aquifer by pumping on day i (mm).

The shallow aquifer contributes base flow to the main channel or reaches within the sub-basin. The steady-state response of groundwater flow to stream flow is,

$$Q_{gw} = \frac{8000 * K_{sat}}{L_{gw}2} * h_{wtbl} \quad (2.7)$$

Where, Q_{gw} is the groundwater flow or base flow into the main channel on day i (mmH_2O), K_{sat} is the hydraulic conductivity of aquifer(mm/day), L_{gw} is the distance from the ridge or sub basin divide for the groundwater system to the main channel(m) and h_{wtbl} is the water table height(m).

Flow routing

Two options are available to route the flow in the channel network: the variable storage and Muskingum methods. The variable storage method uses a simple continuity equation in routing the storage volume, whereas the Muskingum routing method models the storage volume in a channel length as a combination of wedge and prism storages (Arnold *et al*., 1995).

For a given reach segment, storage routing is based on the continuity equation:

$$V_{in} - V_{out} = \Delta V_{stored} \quad (2.8)$$

Where, V_{in} is the volume of inflow during the time step ($m^3 H_2O$), V_{out} is the volume of outflow during the time step ($m^3 H_2O$) and ΔV_{stored} is the change in the volume of storage during the time step ($m^3 H_2O$).

2.3.3. Application of SWAT model in the worldwide

Various studies have been conducted in different parts of the world for simulating hydrology of the watershed. Some of these are described below.

Shrestha *et al*. (2015) used the SWAT model to analyze the impact of land use changes on runoff and sediment yield in Da River Basin of Hoa Binh province, northwest Vietnam. The results showed that SWAT was adequately capable of simulation of runoff and sediment yield as depicted from Nash-Sutcliffe Efficiency, percentage bias and Observation's Standard Deviation Ratio values. Vegetation significantly affects the runoff and sediment yield of the area.

The study by Shimaa (2015) in this study the Arc SWAT interface implemented in the Arc GIS software was used in order to model the hydrology of Simlydam watershed area. SWAT model was successfully calibrated. Manual calibration has been performed first on annual basis followed by monthly basis. The calibration and validation of the model produced good simulation results. The efficiency of the model has been tested by a coefficient of determination, Nash-Sutcliffe Efficiency (NSE) in addition to another two recommended static coefficients: Percent Bias and RMSE observation standard deviation ratio.

The study by Golmar *et al*. (2017) they concluded that a good agreement was also found between the simulated and recorded hydrographs. Temporal variation in the flow generating areas for individual events using the SWAT model and in a modified precipitation index method was performed. A good agreement between the two methods demonstrates the suitability of the SWAT model for estimating time-varying runoff generating areas across a watershed.

Donizete *et al*. (2016) they concluded that the SWAT model showed the potential to simulate the hydrological variables analyzed: maximum and minimum annual daily stream flows and minimum reference stream flows for water use rights. The hydrological variables simulated by the SWAT model did not statistically differ from those observed at a 5% probability level, which qualifies the model for simulations of maximum stream flows associated with different return times, important for hydraulic projects, and to simulate reference stream flows, important to assess the water availability and for irrigation projects.

2.3.4. Application of SWAT model in Ethiopia

The SWAT model was calibrated and validated in some parts of Ethiopia, frequently in the Blue Nile Basin. The study by Mamo and Jain (2013) revealed that the model performance evaluation coefficients shown in this study can be considered reasonably satisfactory and the SWAT model is capable of predicting runoff and sediment yields from Gumera catchment with limited data availability.

The other study by Welde and Gebremariam (2017) in Tekeze Dam watershed, northern Ethiopia, reported that the applicability of the SWAT model in simulating sediment discharge and stream flow dynamics of Tekeze Dam catchment has validated based on the satisfactory values of the statistical measures of the model efficiency. Hence, the model simulation results provide confidence for the further application of the model to assess the hydrologic response analysis due to the spatial and temporal variability of the catchment characteristics will have minimal bias within Tekeze Basin.

A study conducted by Yesuf *et al*. (2015) in Maybar gauged watershed northeast Ethiopia, in this study the well-established, continuous time, long-term, process-based watershed scale Arc SWAT model, in combination with the Arc GIS interface Arc SWAT and SUFI-2 calibration procedure was successfully applied to quantify modeling of sediment yield at a monthly time-step in Maybar hydrometric station.

Ayana *et al*. (2014) used SWAT model in Fincha watershed, the Blue Nile to predict the effects of land use and management practices on runoff and sediment yields. The model gave a satisfactory estimation of runoff and sediment yield as depicted from the calibrated results.

2.3.5. Application of SWAT model in the Gidabo River Basin

According to Mechal *et al*. (2015), recharge variability and sensitivity to precipitation and temperature were studied by applying the hydrological model SWAT (Soil Water Assessment Tool). The long-term average recharge estimated by SWAT model showed a strong spatial variability and revealed a remarkable decrease from the highland towards the rift floor reflecting the large differences in climatic conditions as well as soil and land use characteristics.

The study by Zewude (2016) the hydrological modeling result showed that the SWAT model simulated the runoff satisfactorily. Performance of the model for both the calibration and validation watershed was found to be reasonably very good with Nash-Sutcliffe coefficient (NSE) and coefficient determination (R^2). Therefore, this indicated that the SWAT model performed well for the simulation of the hydrology of the watershed.

Shanka (2017) concluded that Soil and Water Assessment Tool(SWAT) was successfully used to simulate, the impact of climate change on the runoff of Gidabo River Basin were assessed based on projected climate conditions by using GCM outputs of HadCM3 A2a and B2a emissions scenarios with Statistical Downscaling (SDSM) model. This is proved during calibration and validation period of the model performance criterion such as a regression coefficient was used to evaluate the model.

2.4. Methods for Separating the Impacts of LULC and Climate Change on Stream flow

Numerous studies have attempted to quantitatively analyze the impacts of climate change and human activities on runoff changes in recent years (Li *et al*., 2009; Miao *et al*., 2011; Zeng *et al*., 2015; Zhao *et al*., 2014). So far, the methods used fall mainly into three groups: empirical statistics, elasticity-based methods, and hydrological modeling.

Empirical Statistics establishes a relationship between runoff and a climate variable of interest (usually precipitation) and thus usually requires long-term historical hydro-meteorology data (Wang, 2014). Such methods mainly include regression analyses (Zhao *et al*., 2014), time-trend analyses (Zhang *et al*., 2011), and the double-mass curve method (Gao *et al*., 2011).

Zhao *et al*. (2015) used simple linear regression in their analysis of runoff and sediment load in the Yangtze River between 1953 and 2010 and attributed 72% of the reduction in runoff and 14% of the reduction in sediment load to the effects of climate change.

Kong *et al*. (2016) used residual analysis based on double-mass curves to indicate that 91.7% of the change in net runoff in the Yellow River between 1960 and 2012 was due to human activities. Zhang *et al*. (2016) used multiple linear regressions to evaluate the impacts of climate change and human activities on runoff changes in the Poyang River between 1955 and 2009. They estimated that climate change was the main driver (77%) of changes in runoff.

Elasticity-based methods primarily utilize the estimated elasticity in precipitation and potential evapotranspiration to evaluate the effects of climate change. The most widely used elasticity-based methods include the non-parametric method and an analytical method based on the Budyko framework (Budyko, 1974; Dooge, 1992). Ye *et al*. (2013) used the Budyko-Zhang method to distinguish the relative influence of climate change and human activities on changes in stream flow in Poyang Lake between 1960 and 2007. They estimated that climate change-induced changes of 105%-212.1% in runoff relative to the 1960s.

Gao *et al*. (2016) used the Budyko framework to determine the hydrological responses to climate change and human activities in the Jing River Basin during the period 1961-2009. They showed that climate change was the main driver of stream flow reduction, accounting for about 63.9% of the reduction. Mwangi *et al*. (2016) used the Budyko framework to separate out the relative contributions of climate change and land use change to increases in discharge in the upper Mara River in Kenya, and found that changes in land use were the main driver, accounting for 97.5% of the increase, versus 2.5% from climate change.

Hydrological Modeling Method employs complex models to simulate the hydrological cycle. By comparing simulations driven by different climate variable values (whilst keeping the other variables constant), the impact of climate change on runoff variation can be assessed.

Hydrological model, such as the SWAT, TOPMODEL and VIC is comprehensive and based on physical mechanisms that offer a framework to conceptualize and investigate the relationships between climate, underlying surface and hydrological processes in various categories in time and space (Jothityangkoon *et al*., 2001). Hydrological model is more effective as it has related model parameters directly to physically observable land surface characteristics (Legesse *et al*., 2003). Thus, hydrological models can extract a significant amount of information from limited existing data.

The hydrologic modeling approach typically consists of three steps (i) calibrating and validating the selected hydrological model for the target region; (ii) designing and performing OFAT modeling experiments; and (iii) finally comparing the simulated results of different experiments (Zhang *et al*., 2018).

The hydrological model is initially calibrated and validated for the baseline period. Next, the models are run for the variation period without considering any human impacts. Therefore, any differences in simulated runoff before and after the change point are attributable only to climate change, and the contribution of climate change to changes in runoff can, therefore, be expressed as:

Zuo *et al*. (2014) employed a simple hydrological model to identify the impacts of climate change and human activities on changes in runoff in the Jing River Basin and showed that 51% of the runoff decline was due to human activities.

Zeng *et al*. (2015) used the SIMHYD model to separate out the effects of climate change and human activities on surface runoff changes in the Luan River Basin and showed that 46.8% of the runoff changes were due to climate change and 53.2% were due to human activities. Ahn and Merwade (2014) used four hydrological models to quantify jointly influences on stream flow; human-induced stream flow decreases accounted for 74%, 55.5%, 71.4%, and 85.7% of the total decreases in Indiana, New York, Arizona, and Georgia, respectively.

Determination of a baseline period

All the methods described above first require that a baseline period is defined. The calculated contributions to variations in runoff from climate change and human activities are not absolute but instead are calculated relative to this baseline period. Thus, identifying an appropriate baseline period is one of the most important steps in the process. Two methods are commonly used for determining the baseline period. The first is the human-designated method, in which the anthropogenic effects on runoff variation are assumed to be weaker during a pre-selected the earlier period of time. The post-baseline periods are then analyzed relative to this selected earlier period.

Many researchers have applied this method to determine the baseline period. For example, Miao *et al*. (2011) used 1950 to 1969 as the baseline period in a study that quantified the contribution of climate change to decreases in Yellow River stream flow from 1970 to 2008. Similarly, Xu (2007) quantified the relative contribution of anthropogenic activity to hydrological features in the Jialingjiang River Basin from 1981 to 2000 with respect to a baseline period of 1956 to 1980.

A second method of determining the baseline period is the abrupt change method, in which an abrupt change point is detected from the analysis of the statistical characteristics of a long-term hydrological series. The hydrological series is then divided into a pre-change period (the baseline) and a post-change period. Commonly used techniques for assessing the abrupt change point include the Pettit test, the Mann-Kendall test, and the double-mass curve test. Li *et al*. (2007) used the non-parametric Mann-Kendall-Sneyers rank test to determine the baseline period in their study of the effects of climate change and human activities on variations in the runoff in the Wuding River Basin.

Liang *et al*. (2015) used the Pettit test to determine the baseline period in their study of the relative impact of climate change and ecological restoration on stream flow in China's Loess Plateau. During the past decade, the abrupt change point method has been more widely used than the human-designated method.

However, both methods have advantages and disadvantages. The human-designated method selects earlier period as the baseline period, which human activities are small in this period, but it lacks a standard for determining the baseline period, which means that the baseline period can be evaluated only subjectively. Thus, baseline periods determined separately may produce obvious differences and unreliability in the results.

The abrupt change method is the more scientific way of determining the baseline as it is based on a statistical method; however, the relatively frequent human activity may occur during the baseline period. Most researchers tend to apply the abrupt change method (Liang *et al*., 2015; Li *et al*., 2007).

Table 2.1. *Relative merits of the three methodological categories*

Methods	Data used	Advantages	Disadvantages
Empirical statistics	Precipitation	Easy to calculate	Lack physical mechanisms
Elasticity-based methods	Precipitation and potential evapotranspiration	Easy to calculate but with a more physically realistic basis	Potential evapotranspiration is relatively difficulty to monitor; the empirical method could introduce uncertainty
Hydrological modeling	Precipitation, temperature, humidity, sunshine duration, wind speed, land use data, soil data, etc.	Most promising method; includes comprehensive physical processes	Time consuming; requires a large number of input data sets; uncertainties in model calibration and validation

CHAPTER THREE

3. MATERIALS AND METHODS

3.1. Description of the Study Area

Upper Gidabo watershed is one of the tributaries of the Gidabo River Basin. Upper Gidabo watershed is located in Sidama zone of the SNNPRS of Ethiopia. The watershed has an area of 636.23km^2 and covers seven woredas namely: Dale (26.7%), Shebadino (19.5%), Wonsho (25.9%), Aleta wondo (0.1%), Bursa (0.1%), Arbegona (2.5%) and Gorche (25.3%).

The upper Gidabo watershed is bordered on the northwest and South by the Lake Hawassa watershed, on the southwest and South by middle Gidabo River Basin, and on the northeast and southeast by Genale-Dawa River Basin.

In terms of Geographic coordinate system, the watershed lies between 6^{0}40'3"- 6^{0}55'59"North latitudes and 38^{0}21'31"- 38^{0}38'24" East longitudes. The River originates from the northeastern Mountains of Soka Sonicho from Garamba Mountain in Arbegona woreda (Mechal *et al.*, 2015). The altitude of watershed varies within the range of 1679 to 3178m above sea level.

The watershed is characterized by three main seasons. The long rainy season is in the summer from June to September locally it is also known as '*Kiremt'*. The dry period (locally named as '*Bega'*) extends between October to February, and small rainy season is during March, April and May (locally named as '*Belg'*) (NMSA,1996). The mean annual temperature at the upper Gidabo watershed is in the range 10.04c^o to 25.8c^o and the annual rainfall varies between 925mm to 1636mm.

According to soil data of MWIE in upper Gidabo watershed, five main soil types are found which include; Chromic Luvisols (20.60%), Chromic Vertisols (9.79%), Eutric Cambisols (2.04%), Orthic Luvisols (56.17%) and Pellic Vertisols (11.39%). According to Kedir (2002), soils of upper Gidabo watershed can be divided into four textural classes: sandy loam (including the Red and Gray varieties), silty loam, clays and thin gravelly sand soils.

Generally, the watershed is well known by the Agroforestry system. Major types of crops grown in the area include; Coffee, Enset, Avocado, Chat (*Catha edulis*), banana (*Ensete ventricosum*). In some upper parts of the watershed: maize, teff, barley, wheat and small extent pulses and oil crops. In this watershed, some farmers also practice traditional irrigation development activities from perennial rivers and springs. Moreover, livestock production is an important and integral component of the agricultural sector in the upper Gidabo watershed.

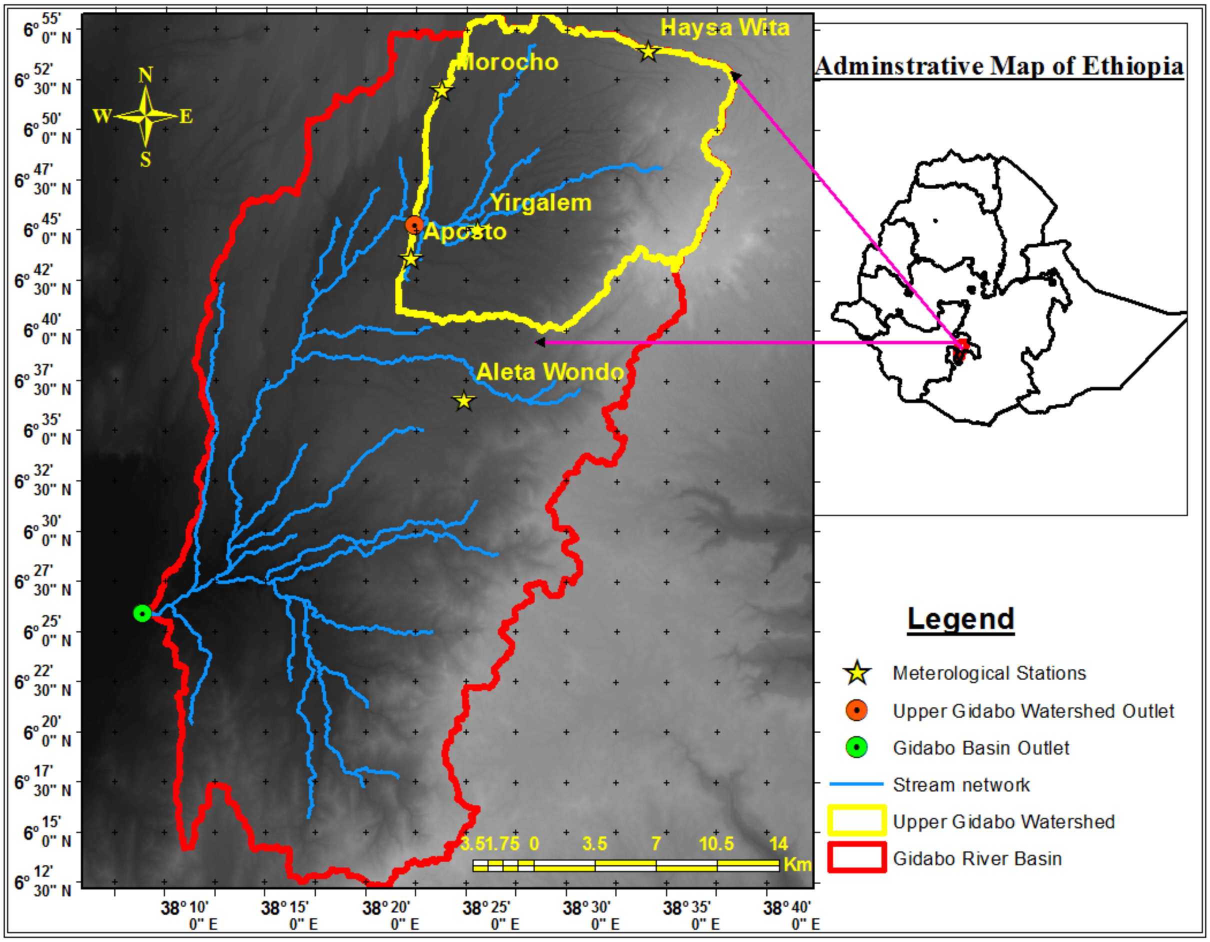

Figure 3.1. *Location map of the study watershed (source: Author)*

3.2. Types and Sources of Data

For this study various data were required that include topographic data (DEM), land use and land cover data, soil data, stream flow data, daily data of climatic variables (daily data of precipitation, maximum and minimum temperature, relative humidity, wind speed and solar radiation). The DEM and land cover satellite data were obtained from the USGS website. Soil and hydrological data were collected from the Ministry of Water Resources and Energy of Ethiopia. The climatic data were obtained from the National Meteorological Agency of Ethiopia and Global weather data for the SWAT website.

Landsat data

This study was done by using Land sat imageries to identify changes in land use and land cover distribution in the upper Gidabo watershed over 32-year period from 1985 to 2016. Land sat images; Landsat-5 TM, Landsat-7 ETM+ and Landsat-8 OLI/TIRS were selected for the period of 1985, 2002 and 2016 respectively. To avoid a seasonal variation in vegetation pattern and distribution throughout a year, the selection of dates of the acquired data were made as much as possible in the same annual season of the acquired years.

Table 3.1. *Characteristics of satellite imagery utilized*

Year	Sensors	Spatial resolution	Acquisition date	Path/row
1985	Landsat-5 TM	30×30m	January 18, 1985	168/85
2002	Landsat-7 ETM+	30×30m	January 25, 2002	168/85
2016	Landsat-8OLI/TIRS	30×30m	January 24, 2016	168/85

The images were obtained from the United States Geological Survey (USGS) Earth Resources Observation Systems (EROS) data center under the Land sat Archive. The years were selected by taking into consideration availability and quality of Land sat images. According to Kindu *et al.* (2015), the images were acquired as much as possible in the same season to avoid the effect of seasonal variations. Other data were also collected for the analyses, including GPS points for major LULC classes, boundary shapefile of the watershed for clipping the Land sat images.

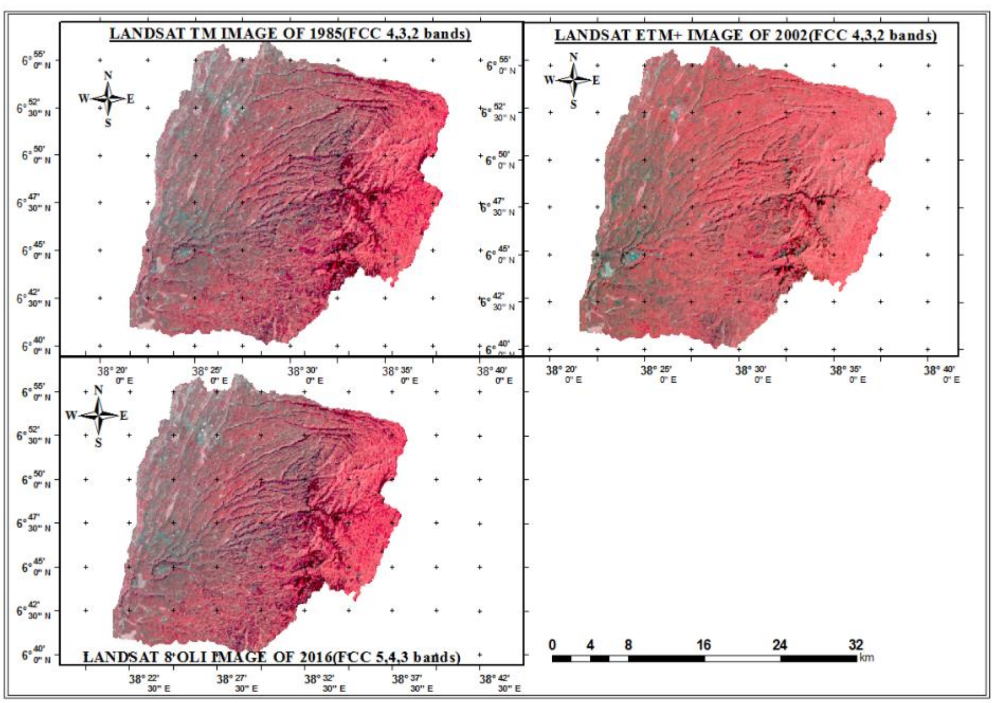

Figure 3.2. *Landsat satellite imagery*

Soil data

Soil data is one of the major input data for the SWAT model with inclusive physical and chemical properties. The soil shapefile of the study area was obtained from the Ministry of Water Resources and Energy of Ethiopia, and physical and chemical properties of soil were extracted from the Harmonized World Soil Database with two layers.

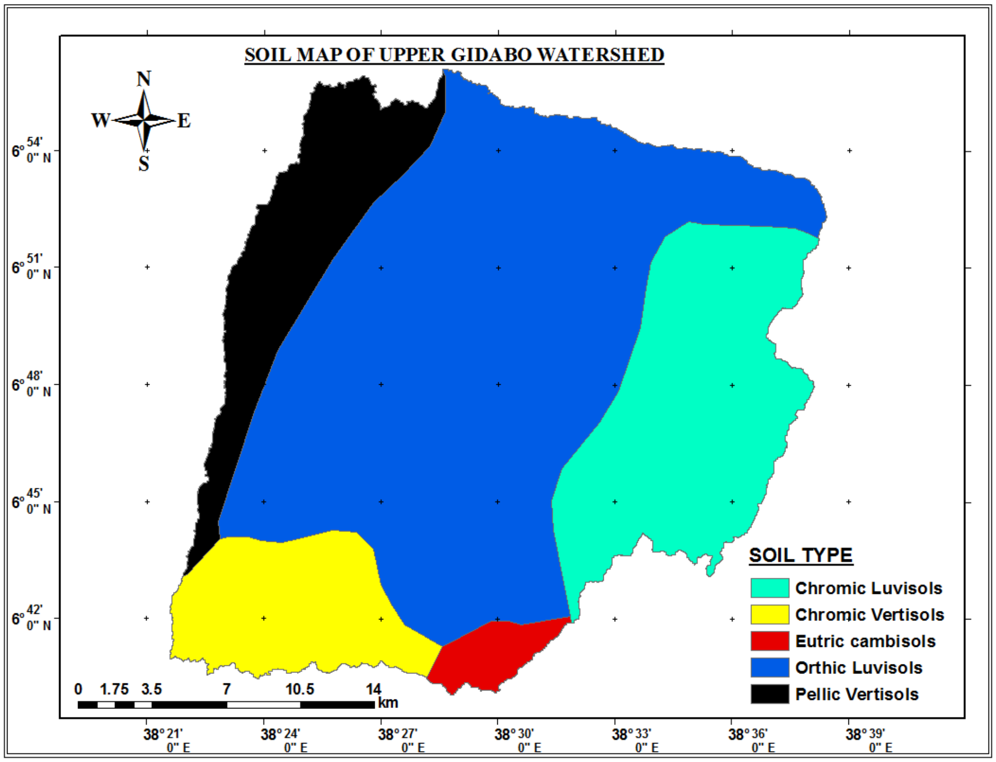

Figure 3.3. *Major Soil types of upper Gidabo watershed*

Table 3.2. *Major Soil types and coverage in upper Gidabo watershed*

№	Soil type		Area coverage	
	Soil name	Textural class	Area km^2	Area%
1	Chromic Luvisols	Sandy clay loam	131.09	20.60
2	Chromic Vertisols	Clay	62.30	9.79
3	Eutric Cambisols	Loam	12.98	2.04
4	Orthic Luvisols	Loam	357.36	56.17
5	Pellic Vertisols	Clay	72.49	11.39
	Total		636.23	100

SWAT model requires soil physical and chemical properties such as soil texture, available water content, hydraulic conductivity, bulk density and organic carbon content etc. for two layers of each soil type. These data were obtained from Harmonized World Soil Database produced by the Food and Agriculture Organization of the United Nations (FAO), the International Institute for Applied Systems Analysis (IIASA) and the Institute of Soil Science and Chinese Academy of Sciences. The soil data include five soil types for the upper Gidabo watershed with two layers (topsoil layer thickness of 300 mm, and sub-soil thickness of 700 mm).

Table 3.3. *Physical and chemical properties of soil in the watershed*

	Soil type									
	Chromic luvisols		Chromic vertisols		Eutric Cambisols		Orthic luvisols		Pellic vertisols	
Soil characteristics	*L1*	*L2*	*L1*	*L2*	*L1*	*L2*	*L1*	*L2*	*L1*	*L2*
SOL_Z(mm)	300	700	300	700	300	700	300	700	300	700
SOL_BD(Mg/m^3)	1.3	1.3	1.6	1.7	1.2	1.3	1.3	1.3	1.3	1.2
SOL_AWC(mm/mm)	0.165	0.165	0.125	0.125	0.175	0.175	0.160	0.160	0.144	0.144
SOL_ZMX(mm)	1000		1000		1000		910		820	
SOL_K (mm/hr.)	12.02	9.7	1.67	1.09	14.05	7.13	10.69	10.19	8.38	11.35
SOL_CBN (%SW)	0.4	0.3	0.6	0.4	1.9	0.7	1.1	0.6	1.3	0.5
CLAY (%)	27	33	55	59	24	30	21	26	43	22
SILT (%)	22	22	30	28	31	32	32	26	29	22
SAND (%)	51	45	15	12	45	38	47	48	28	20
USLE_K	0.265	0.265	0.202	0.202	0.267	0.267	0.289	0.289	0.259	0.259
SOL_ALB	0.227	0.275	0.154	0.227	0.013	0.127	0.059	0.154	0.040	0.187

Note: - *L1* and *L2* are first and second soil layers respectively.

Digital elevation model (DEM) data

Digital Elevation Model (DEM) data is required to calculate the flow accumulation, stream networks, and watershed delineation using SWAT watershed delineator tools. A 30m by 30m resolution SRTM Global Digital Elevation Model data was obtained from the USGS website.

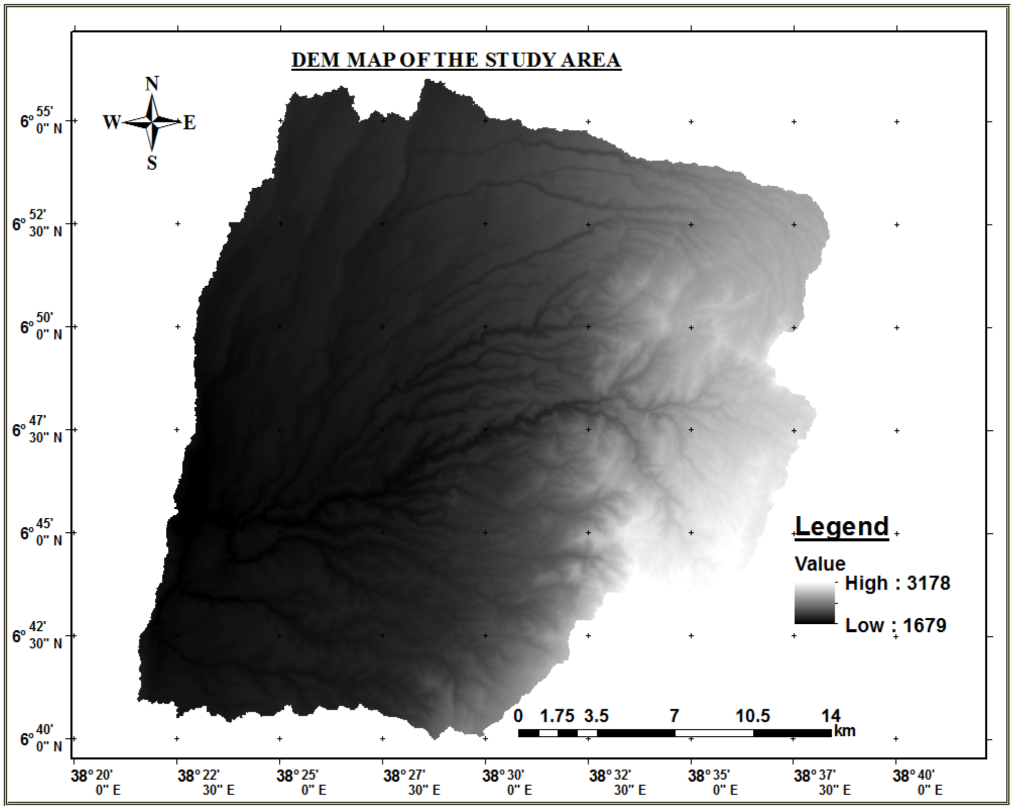

Figure 3.4. *Map of the digital elevation model of the watershed*

Climatic data

The weather variables used for driving the water balance, which includes rainfall, maximum and minimum temperature, solar radiation, relative humidity, and wind speed data. The data were obtained from the Ethiopian National Meteorological Agency (NMA) for five weather stations located within and in close proximity to the watershed; daily rainfall from (Yirgalem, Aposto/Yekatit-25, Aleta Wondo, Morocho/Midregenet and Haysawita); and daily maximum and minimum temperature from (Yirgalem and Haysawita).

Table 3.4. *Metrological stations in and around the watershed*

№	Station name	Latitude(dec.deg)	Longitude(dec.deg)	Total period(year)
1	Morocho(Midregenet)	6.87	38.40	32
2	Aposto/Yekatit-25	6.74	38.37	28
3	Yirgalem	6.75	38.43	31
4	Aleta Wondo	6.61	38.42	32
5	Haysawita	6.90	38.57	32

Among the stations within the watershed, there is no synoptic station that has all weather parameters such as rainfall, maximum and minimum temperature, solar radiation, wind speed and relative humidity. To avoid this problem, the daily meteorological data from 1985 to 2016 were downloaded from Global Weather Data for SWAT.

In order to improve the accuracy of the simulation, daily precipitation and daily maximum and minimum temperature values (1985-2016) from five stations in and around the watershed were used instead of the rainfall and maximum and minimum temperature data from the Global Weather Data for SWAT. Daily solar radiation, relative humidity, and wind speed data were used from Global Weather Data for SWAT.

Stream flow data

The stream flow data of the upper Gidabo watershed is needed for the calibration and validation of the model. The daily stream flow data (1985-2015) is sufficient and were collected from the Minister of Water Resources and Energy of Ethiopia at Aposto river gauging station.

3.3. Software and Tools Used for the Study

For the success of this research, different software and tools were used. Those software and tools with their purpose were indicated in Table 3.5.

Table 3.5. *Software and tools used for the study*

№	Software and tools	Purpose
1	Arc GIS 10.3.1	Spatial data processing and to run arc SWAT software
2	Arc SWAT 2012_10.3.19	Hydrologic modeling purpose
3	ERDAS imagine 2014	LULC map classification and interpretation
4	XLSTAT 2017	Climatic trend analysis
5	Google earth	Classified image accuracy assessment
6	SPSS 20	Hydrologic missing data analysis
7	Rainbow 2.2	Climatic data homogeneity test
8	MS Excel and Word 2013	Writing and graphing and calculations
9	GPS Garmin 78	Collecting accuracy assessment points
10	SWAT-CUP 5.1.6.2	Model Calibration, sensitive analysis and validation

3.4. Methodology

This study was carried out in four steps. First, land use and cover maps for the years 1985, 2002 and 2016 were produced to examine the land use and cover change. Secondly, the climatic variables trend analysis was done by using Man-Kendall trend test. Thirdly, the SWAT input parameters were prepared and simulation run was carried out, and a sensitivity analysis was performed to identify parameters that influence the predicted stream flow the most, the efficiency of the model was assessed by comparing simulated and observed monthly stream flow. Finally, the contribution of LULCC and climate change on stream flow reduction analysis was done by using hydrologic modeling approach of one factor at a time (OFAT) scenarios.

3.5. Data Analysis

3.5.1. Landsat image analysis

Landsat image pre-processing

The images used in this study area were Orthorectified to a Universal Transverse Mercator projection using datum WGS84 zone 37N. The images were geometrically and radiometrically corrected. Pre-processing of the images like clipping and layer stacking task were performed before the beginning of the actual classification. Moreover, all the acquired satellite images were enhanced using histogram equalization to improve image quality.

Image classification

The Land use and land cover change studies usually need the development and the definition of homogeneous land use and land cover units before the analysis is started. These have to be differentiated using the available data source such as remote sensing, any other relevant information and the previous local knowledge.

Based on the satellite images and training points the land use and land cover classes analyzed for changes were: Grazing Land, Mixed forest, Evergreen forest, Agricultural land and Settlements/built-up areas. Categorizing the above listed LULC classes was done based on visual interpretation of the satellite images and field observation, as well as Google earth imageries were used.

Table 3.6**.** *Description of the land use classes in the study area*

№	LULC classes	Description
1	Agricultural land	Areas used for both annual and perennial crop cultivation, homestead Agroforestry systems and the scattered rural settlements that are closely associated with largely sized cultivation fields due to the difficulty encountered in identifying the dispersed rural settlements.
2	Evergreen forest	It includes the area of land covered with sparsely populated forest, riverine trees and artificially planted indigenous and non-indigenous groups of trees like *eucalyptus globule*, *eucalyptus comanduleses*, *cordia Africana* and others.
3	Mixed forest	Grassland that refers to those land units that are used for livestock grazing including privately and communal owed grazing land areas. The land is basically covered by grass and herbaceous species.
4	Grazing land	Land areas covered by dense trees and thick vegetation forming a closed canopy. This describes the areas with evergreen trees mainly growing naturally in the reserved land along the rivers and on the hills area.
5	Built-up area	Land areas included in this category are: residential, commercial, industrial, transportation, roads and mixed urban built-up areas are comprised of low residential areas of scattered housing, dense residential areas and little areas and infrastructure.

Image classification is the process of assigning pixels of a continuous raster image to the predefined land cover classes. It is always a difficult and time-consuming task. A different issue to keep in mind to avoid overlapping features and finish with effective classification is parallel with the ground truth. The result of the classification is mostly affected by various factors such as classification methods, algorithms, collecting of training sites etc.

In remote sensing, there are various image classification methods. The inappropriateness depends on the purpose of land cover maps produced for and the analyst's knowledge of algorithms is using. However, in most cases, the researchers categorized them into three major categories: Supervised, unsupervised and hybrid.

For this study, the supervised classification type was applied. It is the most common type of classification technique in which all pixels with similar spectral value are automatically categorized into land cover classes or themes. Supervised classification was used, which relies on the prior knowledge of pattern recognition in the study area. It requires the manual identification of a point of interest areas as a reference or ground truth within the images to determine the spectral signature of identified features.

For this study, the land cover map was produced based on the pixel-based supervised classification through the steps such as selecting the training sites which are typically representative of the land cover classes. The training sites were collected based on the analyst's personal experience and knowledge of the physiographical knowledge of the area. In addition, image enhancement and composition were applied for better discriminating the land cover classes.

The references used to select the training sites for the supervised image classification was the Google earth high-resolution imagery and ground control points. Training areas were derived by connecting ERDAS Imagine 2014 software with Google Earth and then determine the cover type by examining the image on Google Earth for each color having the same cluster from the satellite image. Using this approach around 140 training points were collected from each image (1985 and 2002) and, for 2016 image classification 140 points were collected by using GPS Garmin-78. Finally, the classification was performed using the supervised classification method.

Accuracy assessment

Accuracy assessment is an important step in the image classification process. The objective of this process is to determine quantitatively how effectively pixels were grouped into the correct features classes in the area under investigation. It is a process used to estimate the accuracy of image classification by comparing the classified map with a reference map (Caetano *et al*., 2005). The most widely used classification accuracy is in the form of error matrix, which can be used to derive a series of descriptive and analytical statistics (Manandhar *et al*., 2009).

The columns of the matrix show the number of pixels per class for the reference data, and the rows show the number of pixels per class for the classified image. From this error matrix, the number of accuracy measures such as overall accuracy, user's and producer's accuracy determined. The overall accuracy is used to indicate the accuracy of the whole classification (i.e. number of correctly classified pixels divided by the total number of pixels in the error matrix), whereas the other two measures indicate the accuracy of individual classes.

Overall accuracy

The overall accuracy gives the overall results of the error matrix. It is calculated by dividing the total number of correct pixels (diagonals) by the total number of pixels in the error matrix. According to Anderson *et al*. (1976), the minimum accuracy value for a reliable land cover classification is 85 %.

$$OA = \frac{Sd}{n} * 100 \tag{3.1}$$

$OA$is overall accuracy, Sd is sum of values along diagonal and n is total number of sample location.

Producer's accuracy

The producer's accuracy tells us how well a certain area can be classified. It is obtained by dividing the number of correctly classified pixels in the category by the total number of pixels of the category in the reference data. It gives only the proportion of correctly classified pixels. The overall result of the producer's accuracy ranges from 82.5 % to 95%. The lowest values were misclassified due to the similar spectral value of different land cover classes. For instance, evergreen forest with mixed forest and agricultural land with mixed forest.

$$PA = \frac{Ci}{Ct} * 100 \tag{3.2}$$

PA is producers accuracy, Ci is correctly classified sample in column, Ct is total number of sample location.

User's accuracy

It is the ratio between the total number of pixels correctly belonging to a class (diagonal elements) and the total number of pixels assigned to the same class by the classification procedure (row total). This quantity explains the probability that a pixel of the classified image truly corresponds to the class to which it has been assigned

$$UA = \frac{Ri}{Rt} * 100 \tag{3.3}$$

UA is users accuracy, Ri is correctly classified sample location in row, Rt is total number of sample location in row.

The accuracy assessment of the classified map is the comparison of the classified image and the sampling points from the Google Earth Imageries and existing land cover maps (Yesserie, 2009). In this study, the assessment was carried out using 1985 maps and 2002 maps together with the historic Google Earth image and previous knowledge of the area was used as reference data to generate testing data set, and for 2016 image, GPS points were collected for each class.

Land use/cover code according to the SWAT model

Land use is one of the highly influencing the hydrological properties of the watersheds. It is one of the main input data of the SWAT model to describe the Hydrological Response Units (HRUs) of the watersheds.

The SWAT model has pre-defined four-letter codes for each land use category. These codes were used to link or associate the land use map of the study area to SWAT land use databases. Hence, while preparing the lookup-table, the land use types were made compatible with the input needs of the model.

Table 3.7. *LULC classification of the watershed as per SWAT model*

№	LULC classes	LULC class for SWAT	SWAT code
1	Agricultural land	Agricultural Land-Generic	AGRL
2	Mixed forest	Forest-Mixed	FRST
3	Grazing land	Pasture	PAST
4	Evergreen forest	Forest-Evergreen	FRSE
5	Settlements/Built-up area	Residential	URBN

3.5.2. Climatic trend analysis

Rainfall data consistency test

Before consistency test analysis, the normal ratio method was adopted to fill rainfall missing data. The consistency and continuity of rainfall data are very important in statistical analysis such as time series analysis. Both consistency and continuity may be disturbed due to change in observational procedure and incomplete records (missing observations) which may vary in length from one or two days to decades of years.

The missing data are estimated by;

$$P_A = \sum_{i=1}^{n} \frac{NR_A}{NR_i} * P_i \quad (3.4)$$

Where, P_A is precipitation at missing location A, NR_A is the normal monthly or seasonal RF at station A, NR_i is the normal monthly or seasonal RF at station i and n is the number of surrounding station.

In this study, inconsistency in a rainfall record was identified by double mass curve analysis. The double mass curve is a well-known simple tool for checking and adjusting inconsistencies in hydrological data caused by changes in observation methods or data processing. The plotted points tend to fall along a straight line under conditions of homogeneity. The theory of double mass curve is based on a graph of cumulative amounts of the station under consideration against the cumulative amounts of a set of neighboring stations during the same period. If the processing is homogeneous, the graph plots a straight line. Time series analysis of rainfall data before using rainfall records at a station for any analysis, the data has to be checked for continuity and consistency. If the significant change in the regime of the curve is observed, it should be corrected by using:

$$P_{CX} = \frac{P_X M_C}{M} \quad (3.5)$$

Where, P_{CX} is corrected precipitation at station x, P_X is original recorded precipitation at station x, M_C is corrected slope of the double mass curve, M is original slope of the double mass curve. The cumulative data of all stations and each station were presented in Appendix 7.

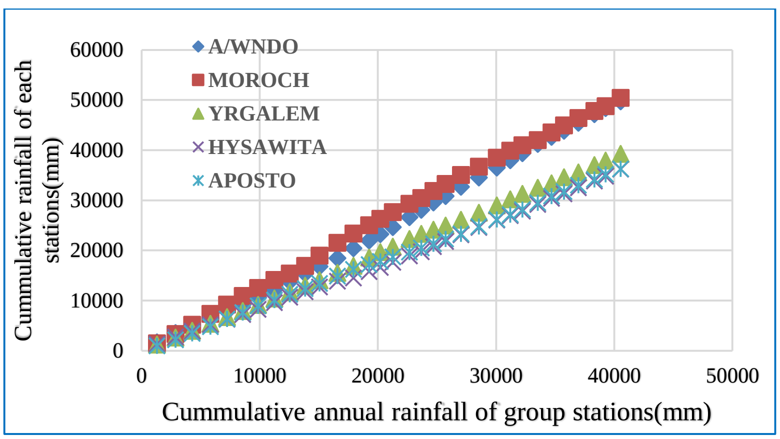

Figure 3.5. *Consistency test for rainfall stations*

Mann-Kendall (MK) statistical test

The non-parametric Mann-Kendall's test (Mann, 1945; Kendall, 1975) developed by H.B. Mann and M.G. Kendall is used to detect trends of annual stream flow, precipitation, and mean temperature in the upper Gidabo watershed.

The Mann-Kendall (MK) is a rank-based non-parametric method for randomness against a time series trend. It is a strong method to avoid the influence of extreme values and is widely used for trend analysis in hydrology and climatology (Belihu *et al*., 2018; Hamed, 2008; Tao *et al*., 2016; Tesemma *et al*., 2010; Yang *et al*., 2017). This method is not only simple to use but it is also resilient to the skewed distribution, missing values and values that fall outside the detection limit, and to the non-stationary nature of data.

The Mann-Kendal trend test was used in this study to investigate trends in the climatic and stream flow variables considered. The test was based on S statistics and each paired observed values x_j (j > k) of the random variable were inspected to find out whether $x_j > x_k$ or $x_j < x_k$.

The Mann-Kendall S Statistic is computed as follows:

$$S = \sum_{k=1}^{n-1} \sum_{j=k+1}^{n} sgn(x_j - x_k) \quad (3.6)$$

Where, x_j and x_k are the annual values in years *j* and *k*, *j* >*k*, respectively, and n is the length of the data set. If the value of S is positive, there is upward trend and vice versa.

$$sgn(x_j - x_k) = \begin{cases} 1 \; if \; x_j - x_k > 0 \\ 0 \; if \; x_j - x_k = 0 \\ -1 \; if \; x_j - x_k < 0 \end{cases} \quad (3.7)$$

The variance of S is,

$$VAR(S) = \frac{n(n-1)(2n+5)}{18} \quad (3.8)$$

The statistic S is approximately normal distributed provided that the following Z transformation is employed:

$$Z = \begin{cases} \frac{S-1}{\sqrt{\sigma}} if \; S > 0 \\ \frac{S-1}{\sqrt{\sigma}} if \; S = 0 \\ \frac{S+1}{\sqrt{\sigma}} if \; S < 0 \end{cases} \quad (3.9)$$

The Mann-Kendal trend test was used in this study to investigate trends in the climatic and stream flow variables considered. The test was based on S statistics and each paired observed values.

The presence of a statistically significant trend is evaluated using the Z value. A positive and negative value of Z indicates an upward (downward) trend. The statistic Z has a normal distribution. To test for either an upward or downward monotonic trend (a two-tailed test) at α level of significance, H_o is rejected if the absolute value of Z is greater than $Z_{1-\alpha/2}$, where $Z_{1-\alpha/2}$ is obtained from the standard normal cumulative distribution tables. For this study, confidence level of 95% was determined by the test statistics.

For significant trends the magnitude of changes was analyzed by estimating slope (*β)*; thus β can be defined as:

$$\beta = median\left[\frac{x_{j-}x_k}{j-k}\right] \qquad (3.10)$$

Where, j>k and β is a robust estimate of the slope.

The trend analysis for annual precipitation

The trend analysis for annual precipitation was done based on observed data from rainfall stations in and around the watershed. There are five rainfall meteorological stations, among those four stations (Yirgalem, Morocho/Midreget, Haysawita, Aposto/Yekati-25 are in watershed boundary and the only one (Aleta Wondo) station is found around the watershed.

The trend analysis for mean annual temperature

The time series of mean annual temperature from two meteorological stations (Haysawita and Yirgalem) was used for temperature trend analysis. These stations are found within the boundary of the watershed.

The trend analysis for stream flow

For this study, the trend analysis was done based on stream flow at Aposto river gauging station. The mean annual stream flow computed over the period 1985 to 2015 for past 31 years.

3.5.3. The SWAT model setup

Watershed delineation

The watershed and sub-watershed delineation was performed using 30 m resolution DEM data using Arc SWAT model watershed delineation function. First, the SWAT project set up was created. The watershed delineation process consists of five major steps, DEM setup, stream definition, outlet and inlet definition, watershed outlets selection and definition and calculation of sub-basin parameters. Once the DEM setup was completed and the location of the outlet was specified on the DEM. The model automatically calculates the flow direction and flow accumulation. Subsequently, stream networks, sub-watersheds and topographic parameters were calculated using the respective tools.

Hydrologic response units (HRU) analysis

The sub-watersheds were divided into HRUs by assigning the threshold values of land use and land cover, soil and slope percentage. In general, the threshold level used to eliminate the minor land use and land covers in sub-basin. Minor soil within a land use and land cover area and minor slope classes within a soil on the specific land use and land cover area. Following the minor elimination, the area of remaining land use and land covers, soils and slope classes are reapportioned by 10%, 20% and 20% respectively. Therefore, that 100% of the irrespective areas were modeled by SWAT.

Land use, soil and slope characterization for the sub-basins were performed using commands from the HRU analysis menu on the arc SWAT toolbar. These tools allowed loading land use and soil maps, which are in raster format into the current project, evaluates slope characteristics and determining the land use/soil/slope class combinations in the delineated sub-watersheds.

Weather generator

In developing countries, there is a lack of full and realistic long period of climatic data. Therefore, the weather generator solves this problem by generating data from the observed one (Danuso, 2002). The Model requires the daily values of all climatic variables from measured data or generated from values using monthly average data over a number of years. The SWAT model contains a weather generator model called WXGEN (Shapley and Williams, 1990).

It is used in the SWAT model to generate climatic data or to fill missing data using monthly statistics, which is calculated from existing daily data. From the values of weather generator parameters, the weather generator first separately generates precipitation for the day. Maximum temperature, minimum temperature, solar radiation and then relative humidity are generated. Lastly, the wind speed is generated independently. For this study, the CFSR weather generator for Ethiopia, prepared for upper Gidabo watershed was used because there is no synoptic weather station in the watershed.

3.5.4. The model calibration, validation, sensitivity and uncertainty analysis

Calibration and validation

SWAT-CUP was developed by Eawag Swiss Federal Institute to analyze the prediction uncertainty of SWAT model calibration and validation results. It provides the user to make a choice between a number of algorithms to perform the calibration such as Sequential Uncertainty Fitting version.2 (SUFI-2), Generalized Likelihood Uncertainty Estimation (GLUE), Markov Chain Monte Carlo (MCMC), and Parameter Solution (ParaSol).

SWAT parameters were calibrated using monthly discharge data from the Aposto station for a period of five years (2006-2010) and then validated using the monthly discharge data of five years (2011-2015). Several iterations of 500 simulations each were carried out for the calibration period of 2006-2010 for monthly flows by adjusting the sensitive parameters obtained through sensitivity analysis until the shapes of predicted and measured stream flows were found to be in reasonable agreement and the criteria of objective functions are satisfied.

Sensitivity analysis

After an initial SWAT simulation was performed, a sensitivity analysis was performed to highlight basin specific parameters that drive model simulations and create sensitivities to model outputs (Arnold *et al*., 2012). Highlighting sensitive parameters was necessary for calibration to assess over and underestimation of output variables. Sensitivity analysis was conducted using SWAT-CUP and a chosen algorithm, the Sequential Uncertainty Fitting version.2 (SUFI-2) algorithm was used. SUFI-2 was chosen to produce practical results, as simulations are not dependent on previous iterations (Srinivasan, 2015).

Sensitivity analysis was used to recognize the parameters that do or do not have the significant influence on the model simulation and identify the most sensitive parameter for model calibration. The most sensitive parameters correspond to the greater change in the output response.

A t-test is then used to identify the relative significance of parameters. The sensitivities are estimates of the average changes in the objective function resulting from changes in each parameter while all other parameters are changing. The t-stat is the coefficient of a parameter divided by its standard error. The p-value for each term tests the null hypothesis that the coefficient is equal to zero (no effect). In this analysis the larger, the absolute value of t-stat and the smaller the p-value the more sensitive the parameter.

Initially, eighteen stream flow parameters were considered which were thought to influence outputs. After an initial iteration run of the model, the most sensitive parameters were identified and only those ten parameters were adjusted so that the calibration efficiency can be improved and calibration variances can be minimized in the study area.

Uncertainty analysis

Parameter uncertainty in SUFI-2 accounts for all sources of uncertainties in driving variables (e.g. rainfall), parameters, the conceptual model, and measured data (e.g. observed flow, sediment). The parameter uncertainty was described by a multivariate uniform distribution in a parameter hypercube, while the output uncertainty was quantified by the 95% prediction uncertainty band (95PPU) calculated at the 2.5% and 97.5%levels of the cumulative distribution function of the output variables.

The 95PPU stands for the 95percent prediction uncertainty or P-factor. The 95PPU measured how well the observed data fit into a 95 per cent confidence range of uncertainty from the simulated output. R-factor measures the range of output uncertainty represented by the visual band. A well-calibrated model will have a small R-factor, represented as a thin 95PPU band that houses the observed measurements.

Model performance evaluation

The predictive capacity of the SWAT model for discharge was determined by using three objective functions: The R^2, NSE and PBIAS.

The coefficient of determination (R^2)

A value shows how well a data fit into a statistical model. The range of coefficient of determination lies between 0 and 1. When R^2 is 1, it can be depicted that the regression line perfectly fits the data while R^2 is 0 indicates that the line does not fit the data at all.

$$R^2 = \frac{\left[\sum_i \left(Q_{m,i} - \overline{Q_m}\right)\left(Q_{s,i} - \overline{Q_s}\right)\right]^2}{\sum_i \left(Q_{m,i} - \overline{Q_m}\right)^2 \sum_i \left(Q_{s,i} - \overline{Q_s}\right)^2} \qquad (3.11)$$

Where, R^2 is coefficient of determination, Q is a variable (e.g. Discharge), and m and s stand for measured and simulated, i is the i^{th} measured or simulated data.

Nash-Sutcliffe efficiency (NSE)

The Nash-Sutcliffe model efficiency coefficient is used to show the predictive power of hydrological models. The Nash-Sutcliffe efficiency has a range between -∞ to 1. When efficiency is equal to 1 it indicates a perfect match of estimated discharge with the observed data whereas an efficiency of 0 suggests that the predictions of the model are as accurate as the observed data are meanwhile an efficiency which is less than zero corresponds that the observed mean is a better predictor than the model.

$$NSE = 1 - \frac{\sum_i (Q_m - Q_s)_i^2}{\sum_i \left(Q_{m,i} - \overline{Q_m}\right)^2} \qquad (3.12)$$

Where, NSE is Nash-Sutcliffe efficiency, Q is a variable (e.g. Discharge), m and s stand for measured and simulated respectively and the bar stands for an average.

Percentage bias (PBIAS)

It is the deviation of simulated data from observed data being evaluated, which is expressed as a percentage. The low magnitude values indicate accurate simulation of the model. Percent bias measures the average tendency of the simulated data to be larger or smaller than the observations. The optimum value is zero where low magnitude values indicate better simulations. Positive values indicate model underestimation and negative values indicate model overestimation (Gupta *et al*., 1999).

$$PBIAS = 100 * \frac{\sum_{i=1}^{n} (Q_m - Q_s)_i}{\sum_{i=1}^{n} Q_{m,i}} \qquad (3.13)$$

Where, Q is a variable (e.g. Discharge) and m and s stand for measured and simulated respectively.

Table 3.8. *Recommended performance ratings for model statistics* **(***Moriasi et al., 2007***)**

Performance rating	NSE	PBIAS (%)
Very good	0.75<NSE≤1	PBIAS<±10
Good	0.65<NSE≤0.75	±10≤ PBIAS<15
Satisfactory	0.5<NSE≤0.65	±15≤ PBIAS<25
Unsatisfactory	NSE≤0.5	PBIAS≥25

3.5.5. Separating the impact of climate change and LULCC on stream flow

Separating impacts of land use and land cover change (LULCC) and climate change on hydrology is essential for watershed planning and management. This is typically done via hydrological modeling in combination with the one factor at a time analysis (Zhang *et al*., 2018).

The methodology consists of three steps, as it was mentioned in the section of the literature review part. In the first step, the model was calibrated and validated. Secondly, designing and performing OFAT modeling scenarios and finally comparing the simulated results of different scenarios.

With increasing data availability and rapid development of process-based distributed hydrological models, the hydrological modeling approach that is usually combined with one factor at a time (OFAT) analysis has gradually become one of the most widely used method for isolating hydrological impacts of LULCC from those of climate change (e.g. Guo *et al*., 2016; Li *et al*., 2009; Luo *et al*., 2016; Natkhin *et al*., 2015; Setyorini *et al*., 2017; Shi *et al*., 2013; Yang *et al*., 2017; Yin *et al*., 2017; Zhang *et al*., 2016; Zhang *et al*., 2017).

Determination of baseline period

As mentioned in the literature part, there are two methods to determine the baseline period: The human-designated method and abrupt change method. The human-designated method selects earlier period as the baseline period, which human activities are small in this period, but it lacks a standard for determining the baseline period, which means that the baseline period can be evaluated only subjectively. Thus, baseline periods determined separately may produce obvious differences and unreliability in the results.

The abrupt change method is a more scientific way of determining the baseline as it is based on a statistical method; however, a relatively frequent human activity may occur during the baseline period. Most researchers tend to apply the abrupt change method a long-term hydrological series (Liang *et al*., 2015; Li *et al*., 2007); thus, for this study, the abrupt change method for stream flow data was used to determine the baseline period. The statistical abrupt change point for stream flow data is in 1998. Therefore, baseline period is from 1985-1998 and post change period is from 1999-2016.

Scenarios development

The OFAT (changing one factor at a time either climate or land use keeping other constant) modeling scenarios (S1, S2, S3 and S4) were generally designed through the combinations of *C1*, *C2*, *L1* and *L2*.

Table 3.9. *Scenarios development for LULC and climatic conditions*

Scenarios	Land use condition		Climatic condition	
S1	*L1*	1985 map	*C1*	1985-1998 climate
S2	*L2*	2016 map	*C1*	1985-1998 climate
S3	*L1*	1985 map	*C2*	1999-2016 climate
S4	*L2*	2016 map	*C2*	1999-2016 climate

Note: S1 is scenario for baseline period (pre-change period)

S2 is scenario for changing LULC while holding climate constant

S3 is scenario for changing climate while holding LULC change constant

S4 is scenario for variation period (post change period)

To represent these two periods land cover maps *L1* from 1985s' (1985-1998) and *L2* from the 1999s' (1999-2016) were used. The land use and coverage map for scenarios building and mean annual stream flow simulations should represent two periods, for the first period 1985s' the land use map *L1* is land use map of 1985. For the second period 1999s,' the land use map *L2* is the land use map of 2016.

To calculate the hydrological change induced by LULC and climate change and combined change respectively (Yang *et al.*, 2017) proposed new method. According to that method;

$$\Delta Q_L = \frac{1}{2}[(Q_{L2}^{C1} - Q_{L2}^{C1}) + (Q_{L2}^{C2} - Q_{L1}^{C2})] \tag{3.14}$$

$$\Delta Q_C = \frac{1}{2}[(Q_{L1}^{C2} - Q_{L1}^{C1}) + (Q_{L2}^{C2} - Q_{L2}^{C1})] \tag{3.15}$$

$$\Delta Q = \Delta Q_L + \Delta Q_C = Q_{L2}^{C2} - Q_{L1}^{C1} \tag{3.16}$$

$\Delta Q_L, \Delta Q_C$ and ΔQ are the hydrological change due to land use/cover change, and climate change and combined change respectively. $Q_{L1}^{C1}, Q_{L2}^{C1}, Q_{L1}^{C2}$ and Q_{L2}^{C2} are the mean the annual values of the hydrological components simulated in the scenarios of S1,S2,S3 and S4 respectively.

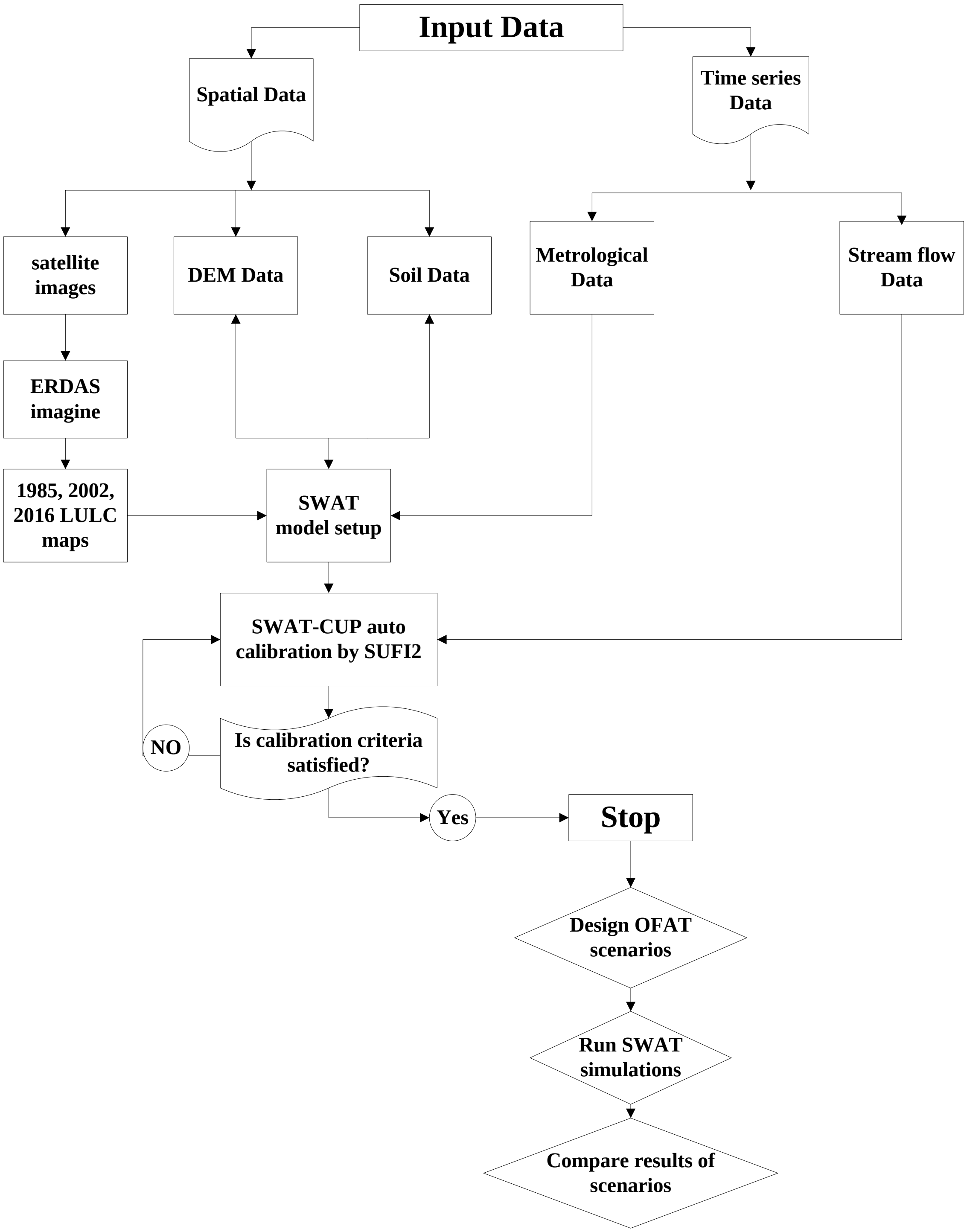

Figure 3.6. *Methodological framework adopted in this study (Source: Author)*

CHAPTER FOUR

4. RESULTS AND DISCUSSION

4.1. Results of Land Use and Land Cover Change

Based on the prior knowledge collected from the people who lived in the study area and through observation of the current situation a classification scheme was developed for the study area. Using the application of image classification methods five major land uses and land cover types were identified in upper Gidabo watershed. These include evergreen forest, agricultural land, and grazing land, mixed forest and settlement /built-up area based on the characteristics of satellite images of the year 1985, 2002 and 2016.

4.1.1. Land use and land cover classification

Land use land cover classification for 1985 image

Based on the classified maps, five (agricultural land, grazing land, evergreen forest, mixed forest and settlement/built-up areas) classes of land use and cover were obtained. The 1985 land use in the upper Gidabo watershed was mainly classified as agricultural land, which takes up about 37.77% (240.29 km^2) of the total watershed area. About 37.22% (236.76 km^2) of the land use was defined as mixed forest and 13.86% (88.15 km^2), 8.10 % (51.52 km^2) and 3.06% (19.44 km^2) were listed as evergreen forest, grazing land, settlement/built-up areas respectively. The details of these land use classification were listed in Table 4.1 and Figure 4.1.

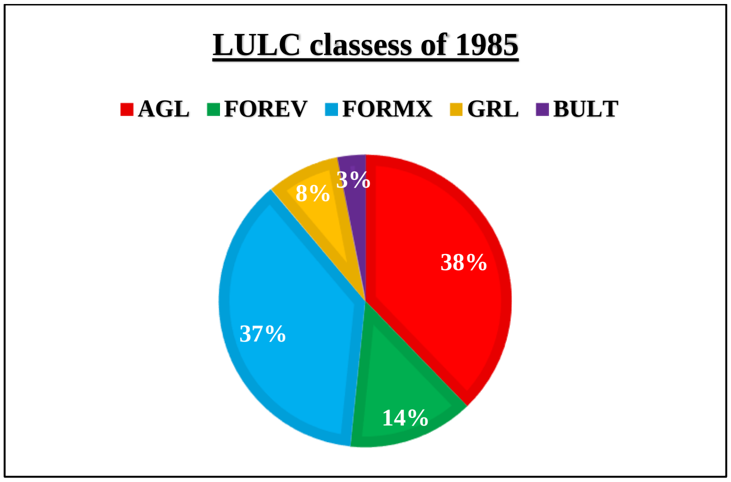

Figure 4.1. *Magnitude of LULC classes for 1985 map*

Table 4.1. *Area of LULC classes and percent of coverage for 1985 map*

№	Land use/cover classes	LULC classes for 1985 map	
		Area(km^2)	Cover (%)
1	Agricultural land	240.29	37.77
2	Evergreen forest	88.15	13.86
3	Mixed forest	236.76	37.22
4	Grazing land	51.52	8.10
5	Settlement/built-up area	19.44	3.06
	Total	636.15	100

Land use and land cover classification for 2002 image

The 2002 land use classification showed that the main type of land use was the agricultural land type, approximately 52.2% of the watershed area (332.04 km^2). About 27.98% (177.96 km^2) of the watershed area was classified as mixed forest. Grazing land, evergreen forest and settlement/built-up land use covered percentages of 12.01% (76.39 km^2), 4.71% (29.94 km^2) and 3.10% (19.74 km^2) respectively of the total watershed area. Table 4.2 and Figure 4.2 presented each land use classification.

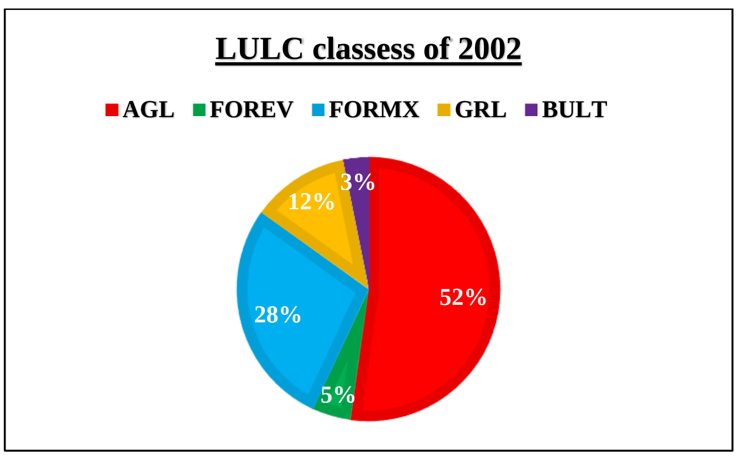

Figure 4.2. *Magnitude of LULC classes for 2002 map*

Table 4.2. *Area of LULC classes and percent of coverage for 2002 map*

№	Land use/cover classes	LULC classes for 2002 map	
		Area(km^2)	Cover (%)
1	Agricultural Land	332.04	52.20
2	Evergreen Forest	29.94	4.71
3	Mixed Forest	177.96	27.98
4	Grazing Land	76.39	12.01
5	Settlement/built-up area	19.74	3.10
	Total	636.08	100

Land use land cover classification for 2016 image

The land use land cover classification for 2016 from Landsat-8 OLI/TIRS satellite image in table 4.3 showed that more than half of the study area was occupied by agricultural land 59.58% (379.07km^2) followed by mixed forest 22.03% (140.18km^2) whereas grazing land, evergreen forest and settlement (built-up area) was occupied; 7.33% (46.66km^2), 5.72% (36.38km^2) and 5.34% (33.96km^2) respectively.

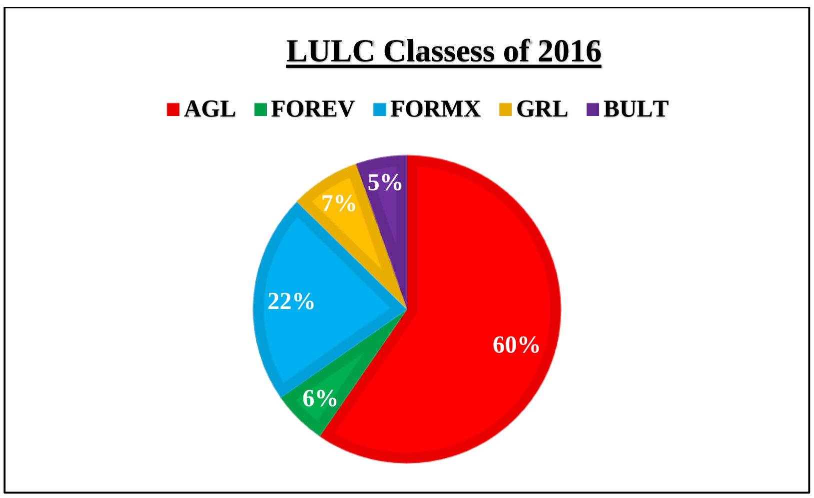

Figure 4.3. *Magnitude of LULC classes for 2016 map*

Table 4.3. *Area of LULC classes and percent of coverage for 2016 map*

№	Land use/cover classes	2016 LULC map	
		Area(km^2)	Cover (%)
1	Agricultural Land	379.07	59.58
2	Forest Evergreen	36.38	5.72
3	Forest Mixed	140.18	22.03
4	Grazing Land	46.66	7.33
5	Settlement/built-up area	33.96	5.34
	Total	636.25	100

From analysis results, the study watershed has undergone various land use and cover changes. Major changes have taken place, particularly in the agricultural areas. The results were presented in form of charts and statistical tables. Table 4.4 and Figure 4.4 showed land use and cover analysis of the study area.

Table 4.4. *LULCC in different periods*

Land use/cover classes	1985		2002		2016	
	Area(km^2)	Cover (%)	Area(km^2)	Cover (%)	Area(km^2)	Cover (%)
Agricultural Land	240.29	37.77	332.04	52.20	379.07	59.58
Forest Evergreen	88.15	13.86	29.94	4.71	36.38	5.72
Forest Mixed	236.76	37.22	177.96	27.98	140.18	22.03
Grazing Land	51.52	8.10	76.39	12.01	46.66	7.33
Settlement/built-up	19.44	3.06	19.74	3.10	33.96	5.34
Total	636.15	100	636.08	100	636.25	100

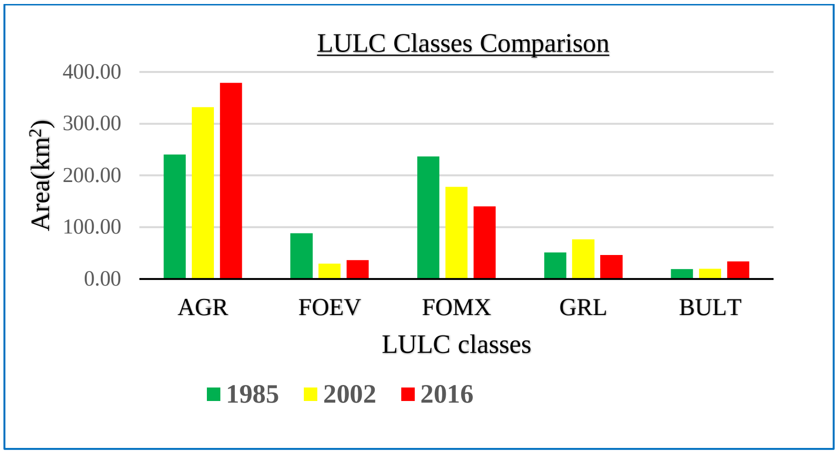

Figure 4.4. *Comparison of magnitude of land use category*

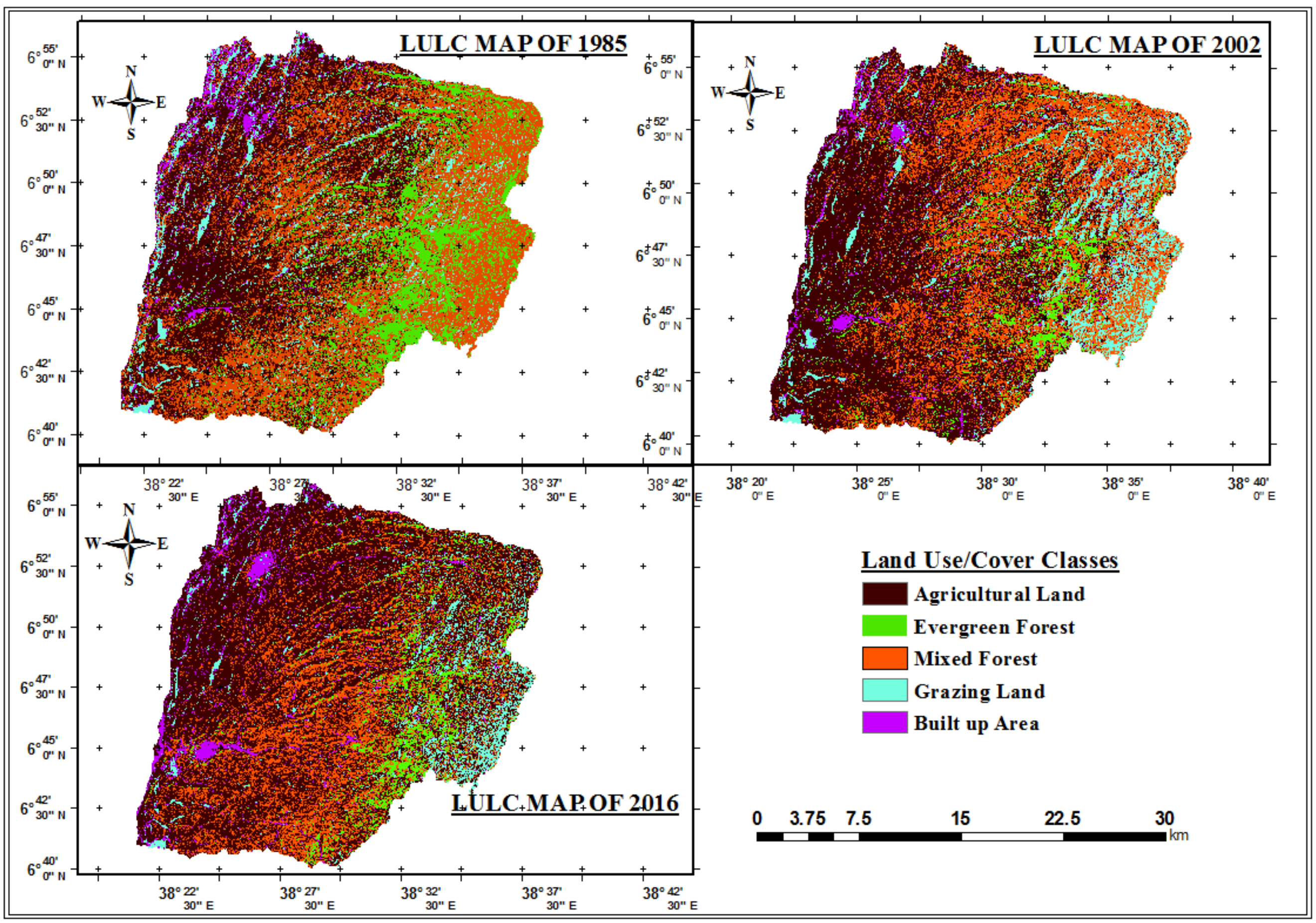

Figure 4.5. *Maps of different year Landsat images in the study watershed*

4.1.2. Land use and land cover change detection

4.1.2.1. Change detection between 1985 and 2002

The lands under Agricultural, settlement/built-up and grazing were increased by 91.76km^2 (38.19%), 0.31km^2 (1.58 %) and 24.87km^2 (48.27%) respectively. Evergreen forest and mixed forest were decreased by 58.20km^2 (66.03%) and 58.80km^2 (24.84%) respectively. This result agreed with the study result by Zewude (2016) in Gidabo River Basin. He showed, during the period of 1986-2000, the agriculture area and built-up area increased to 6.84%, and 1.4% with the rate of change of 1.71% and 0.35% respectively per annum whereas the forest and open shrub land decreased by 0.95% and 0.45% respectively. Generally, there was an increase in agricultural area and built-up areas in this period. This was caused by an increase of deforestation for further settlement and expansion of agriculture.

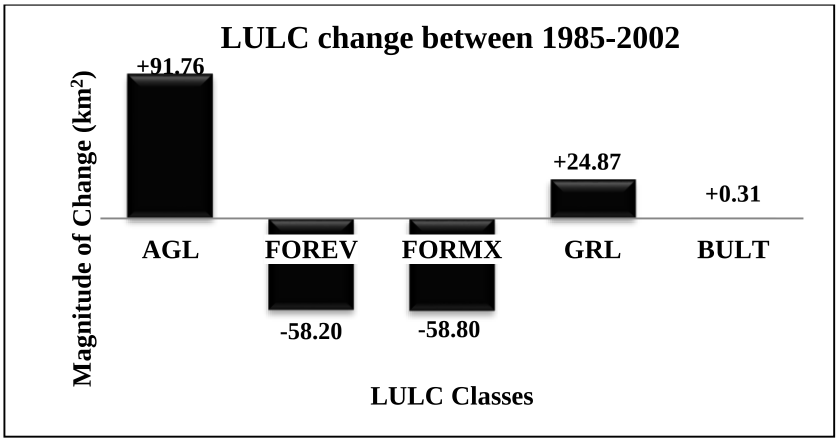

Figure 4.6. *Gross magnitude of change in LULC categories from 1985-2002*

4.1.2.2. Change detection between 2003 and 2016

The lands under Agricultural, Evergreen forest and settlement/built-up were increased by 47.03km^2 (14.16%), 6.44km^2 (21.50 %) and 14.21km^2 (71.98%) respectively. Grazing land and mixed forest were decreased by 29.73km^2 (38.92% and 37.78km^2 (21.23%) respectively. According to the study by Zewude (2016), in Gidabo River Basin, during the period of 2000-2014 the agricultural area and forest area increased by 21.02% and 0.69% respectively. These increases of agriculture area that was due to the expansion of coffee and chat plantation on farmers' farmland whereas evergreen forest increased due to the expansion of area closures around mountainous areas and due to the expansion of different soil and water conservation activities such as afforestation during watershed development programs.

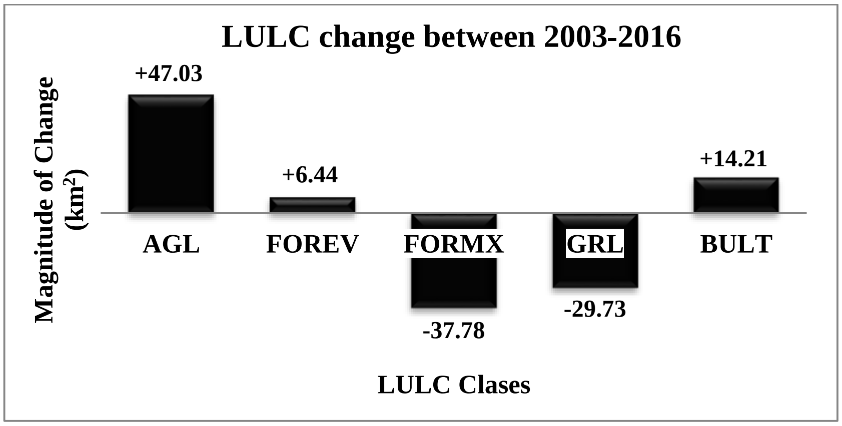

Figure 4.7. *Gross magnitude of change in LULC categories from 2003-2016*

4.1.2.3. Change detection between 1985 and 2016

The lands under Agricultural and settlement/built-up were increased by 138.78km^2 (57.76%) and 14.52km^2 (74.70%) respectively. Evergreen forest, grazing land and mixed forest were decreased by 51.77km^2 (58.73%), 4.86km^2 (9.44%) and 96.58km^2 (40.79%) respectively.

In general, over the past 32 years, agricultural area and built-up area increased. This was resulted from deforestation for further agricultural land expansion and mixed forest decreased due to an increase in fuel wood demand and construction expansion.

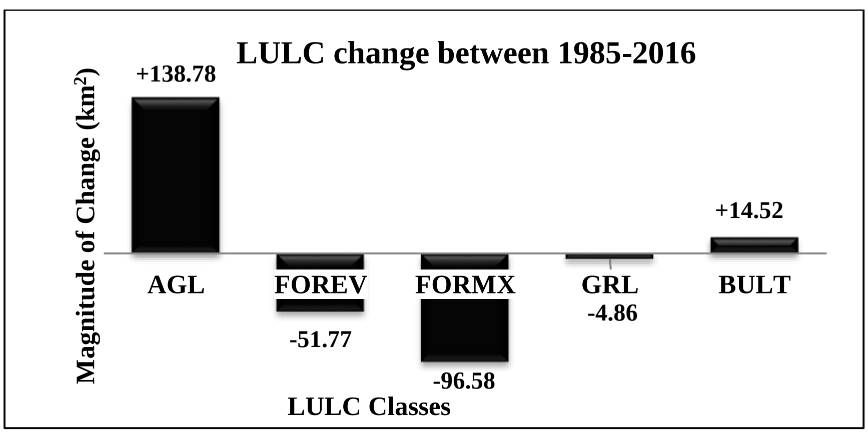

Figure 4.8. *Gross magnitude of change in LULC categories from 1985-2016*

Table 4.5. *Summary of areal extent and change of five LULC classes*

LULC change detection									
LULC Classes	1985-2002, Δyears =18			2003-2016, Δyears =14			1985-2016, Δyears =32		
	ΔArea(km^2)	Change(%)	Annual rate (%)	ΔArea(km^2)	Change (%)	Annual rate (%)	ΔArea(km^2)	Change (%)	Annual rate (%)
AGL	91.76	38.19	2.12	47.03	14.16	1.01	138.78	57.76	1.81
FOREV	-58.20	-66.03	-3.67	6.44	21.50	1.54	-51.77	-58.73	-1.84
FORMX	-58.80	-24.84	-1.38	-37.78	-21.23	-1.52	-96.58	-40.79	-1.27
GRL	24.87	48.27	2.68	-29.73	-38.92	-2.78	-4.86	-9.44	-0.30
BULT	0.31	1.58	0.09	14.21	71.98	5.14	14.52	74.70	2.33

4.1.3. Accuracy assessment of land cover classification

The accuracy assessment was used to determine the correctness of the classified image. It was performed using the error matrix. Using the original mosaic image by combining with the historical Google Earth images as a reference, randomly selected points were compared with the corresponding classification. 140 points for each class were collected for the accuracy assessment of 1985 and 2002 maps respectively. For the land cover map of 2016, 140 points were collected from the field for each class by using GPS. Table 4.6, 4.7 and 4.8 showed an error matrix for the three LULC maps. In this study, the user's accuracy ranges from 76.74% to 100%. The lowest value agricultural lands were to some extent misclassified because of the similarity spectral properties of mixed forest.

Table 4.6. *Error matrix for the classified map of 1985*

Land cover classes(1985)		Reference data						User’s accuracy (%)
		AGL	FOREV	FORMX	GRL	BULT	Row total	
Classified data	AGL	34	0	3	0	0	37	91.89
	FOREV	1	17	1	0	0	19	89.47
	FORMX	3	2	35	2	2	44	79.55
	GRL	1	1	0	18	0	20	90
	BULT	1	0	1	0	18	20	90
	Column total	40	20	40	20	20	140	
	Producer’s accuracy (%)	85	85	87.5	90	90	Overall accuracy (%)=**87.14**	

Table 4.7. *Error matrix for the classified map of 2002*

Land cover classes(2002)		Reference data						User's accuracy (%)
		AGL	FOREV	FORMX	GRL	BULT	Row total	
Classified data	AGL	33	1	6	1	2	43	76.74
	FOREV	0	17	0	0	0	17	100
	FORMX	4	1	34	0	0	39	87.18
	GRL	3	1	0	19	0	23	82.61
	BULT	0	0	0	0	18	18	100
	Column total	40	20	40	20	20	140	
	Producer's accuracy (%)	82.5	85	85	95	90	Overall accuracy (%)=**86.43**	

Table 4.8. *Error matrix for the classified map of 2016*

Land cover classes(2016)		Referenced data						User's accuracy (%)
		AGL	FOREV	FORMX	GRL	BULT	Row total	
Classified data	AGL	37	2	3	2	0	44	84.09
	FOREV	0	18	0	0	0	18	100
	FORMX	1	0	36	0	2	39	92.31
	GRL	1	0	1	18	0	20	90
	BULT	1	0	0	0	18	19	94.74
	Column total	40	20	40	20	20	140	
	Producer's accuracy (%)	92.5	90	90	90	90	Overall accuracy (%)=**90.71**	

4.1.4. LULC transition matrix

Table 4.9 showed a land use and cover transformation matrix for upper Gidabo watershed used to reflect the direction of change in the various land use types. Overall, it was evident that about 377.39 km^2 of lands have changed from all classes, which comprised approximately 59.32 % of the entire area from 1985 to 2016.

This study focused largely on the transformations of agricultural land, mixed, evergreen forest and grassland as these changes are known to affect large areas and may have led to significant alternations in the various hydrological processes. The analysis showed that Agricultural land has increased mainly due to the change over from mixed forest 141.64 km^2, evergreen forest 29km^2 and grassland 30.18 km^2. The study by Zewude (2016) in Gidabo confirmed that the total decrease of a forest has occurred because it was converted to built-up areas and agricultural areas.

Table 4.9. *LULCC matrix of 1985 - 2016*

LULCC matrices		LULC 2016(km^2)					
		AGR	FOREV	FORMX	GRL	BULT	Total(2016)
LULC 1985(km^2)	AGR	161.79	4.50	53.18	3.88	13.91	237.25
	FOREV	29.00	24.20	30.05	3.86	2.78	89.88
	FORMX	141.64	7.24	54.27	25.72	6.50	235.38
	GRL	30.18	0.30	4.32	12.81	5.60	53.21
	BULT	12.83	0.04	1.00	0.88	5.77	20.52
	Total(1985)	375.43	36.28	142.81	47.14	34.56	636.23

4.2. Climatic Trend Analysis Results

4.2.1. Annual rainfall and temperature trend

The results of the Mann-Kendall test and null hypothesis test at 95% confidence level (α=0.05) on the rainfall for the five stations considered in this work. As illustrated in Table 4.10, by running Mann-Kendall test on the number of years for the five stations, the test results in accepting the null hypothesis H_o for most of the stations except for station Morocho (Midregent). Accepting H_o indicates that there is no statistically significant trend in the time series, and the result is statistically insignificant. On the other hand, the values of Z were negative for all stations indicating that the number of rainy year decreases with time.

The value of Sen's slope estimates β and trend statistic Z for annual rainfall recorded at five weather stations from 1985 to 2016 were displayed in Table 4.10. The annual precipitation showed a decreasing trend at all the meteorological stations from 1985 to 2016 and the most decreasing statistical significant trend is observed in Morocho stations (α= 0.05). These results agreed with the study by Belihu *et al*. (2018) in Gidabo River Basin.

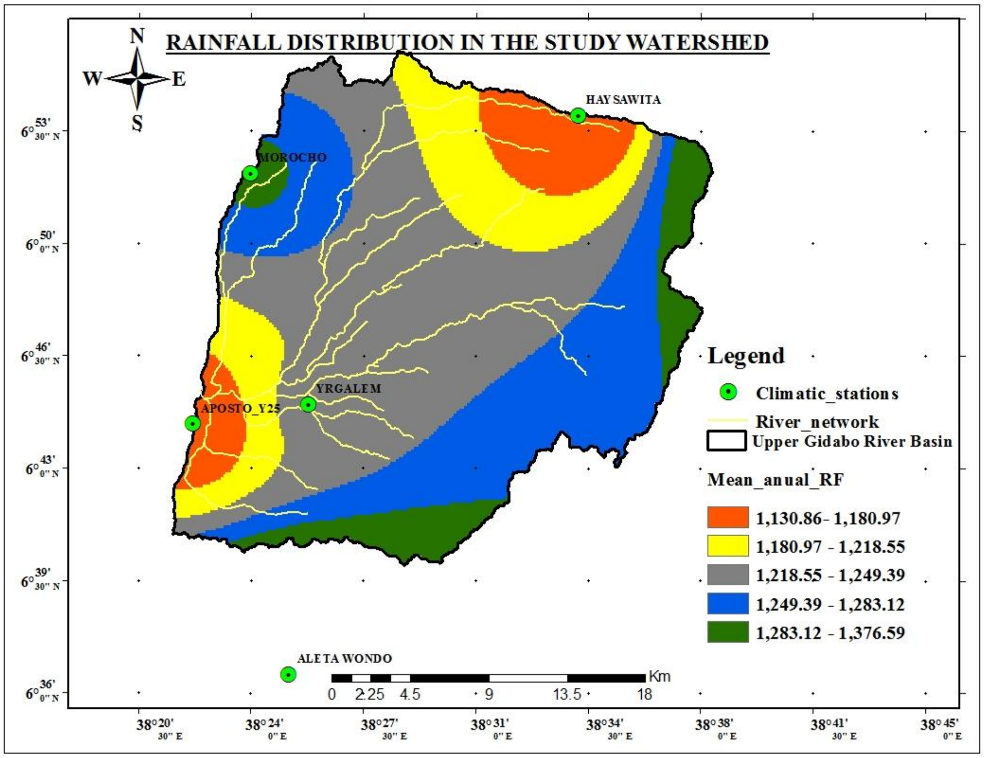

Figure 4.9. *Spatial distribution of mean annual RF(mm)distribution in the study area*

Table 4.10. *Results of the MK test for annual rainfall from 1985 to 2016*

Climatic stations	Annual Total Precipitation		Significance at α=0.05
	Z	β	
Hayisawita	-0.08	-1.14	NS
Yirgalem	-1.29	-3.85	NS
Aposto Yekatit-25	-1.05	-5.82	NS
Morocho(Midregenet)	-4.75	-33.29	SG
Aleta Wondo	-0.41	-2.67	NS

Note: -NS is non-significant and SG is significant

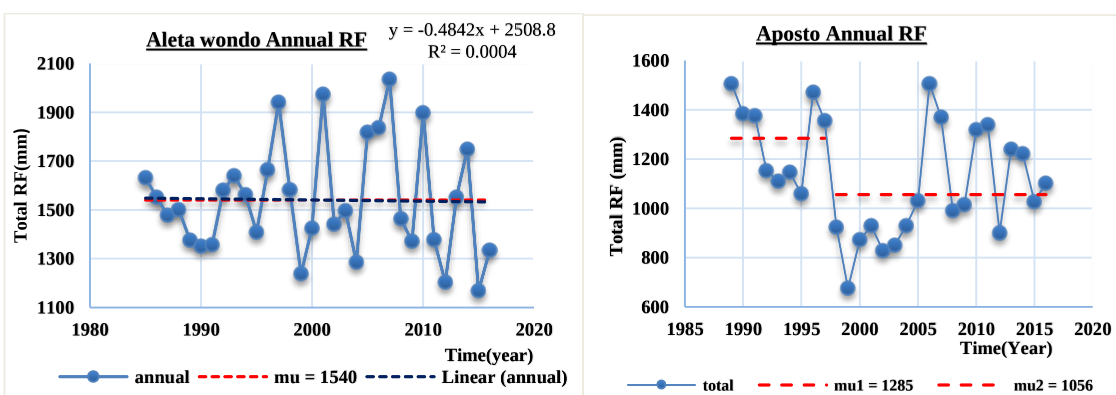

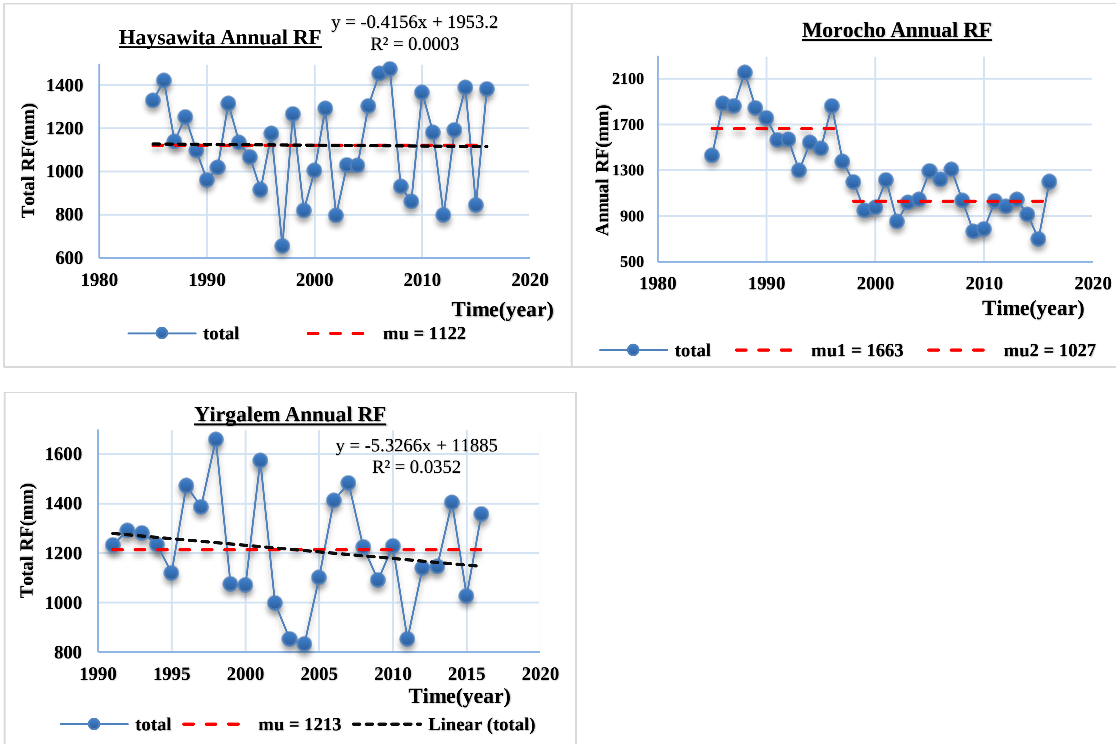

Figure 4.10. *Trends in the annual rainfall over the study period (1985-2016)*

4.2.2. Mean annual temperature trend

The Mann-Kendall test and null hypothesis test at 95% confidence level (α=0.05) for Mean annual maximum and minimum temperature data series, Mann-Kendall test revealed that for both stations (Haysawita and Yirgalem) there was a statistically significant increasing trend in maximum and minimum temperature with Z values 2.74 and 5.69 for Yirgalem station and 4.48 and 4.85 for Haysawita station respectively. The Z values were positive for both stations in the watershed, implying that the mean annual maximum and minimum temperature is increasing significantly in general over the past 32 years.

The study by Belihu *et al.* (2018) the result of temperature analysis revealed that the catchment is getting warmer. In the eastern highlands, the minimum temperature is increasing and on the other hand, the maximum temperature is increasing in the lowlands. The rise in temperature increases the loss of soil moisture both directly and through transpiration. So the runoff amount, which flows toward the stream, was determined by soil moisture status.

Table 4.11. *Results of the MK for annual mean temperature from 1985 to 2016*

Climatic stations	Max. mean annual temp(c°)		Significance at α=0.05	Min. mean annual temp(c°)		Significance at α=0.05
	Z	β		Z	β	
Haysawita	4.46	0.052	SG	4.85	0.052	SG
Yirgalem	2.74	0.054	SG	5.69	0.048	SG

Note: SG=significant

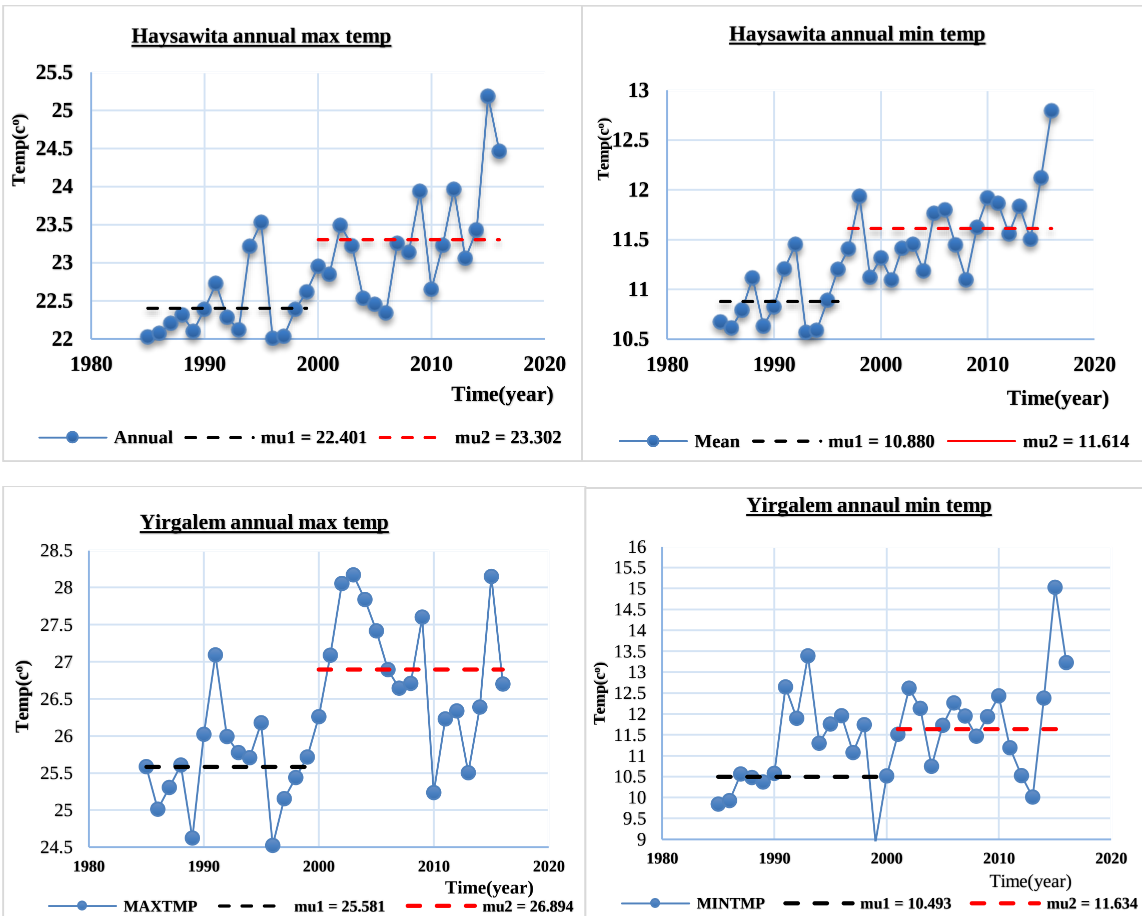

Figure 4.11. *Trends in the mean annual max and min temperature over the study period (1985-2016)*

Note: -Black and red dotted lines show the means in mean annual temperature.

4.2.3. Mean annual stream flow trend

The observed stream flow data from Aposto river gauging station from (1985-2015) was used. In this data, the statistical abrupt change point has occurred from 1998. This abrupt change was caused due to El-Nino effects. The study by Belete (2013) concluded that the Hawassa lake level tends to be high during El-Nino and low during La-Nina. The typical example is the coincidence of extreme historical maximum lake level to the strongest El-Nino events of the century that occurred in 1997/1998. This implies 1997/1998 was the worst El-Nino years in Ethiopia and main Ethiopia rift that caused abrupt reduction change on Gidabo river discharge. The study by Belihu *et al*. (2018) in Gidabo River Catchment using stream flow data at Aposto river gauging station showed that the minimum flow has occurred in 1999 which was about 92.52Mm^3 in terms of volume.

Thus, the entire period 1985-2016 was split into two-time slices i.e.1985-1998 as baseline and 1999-2016 as the post-baseline period. Overall, for the entire available period from 1985-2015 at Aposto river gauging station, the Mann-Kendall's test results showed a decreasing trend for mean annual stream flow. This decreasing trend with Z value is -0.924 at α =0.05 is statistically insignificant with β value -12.79.

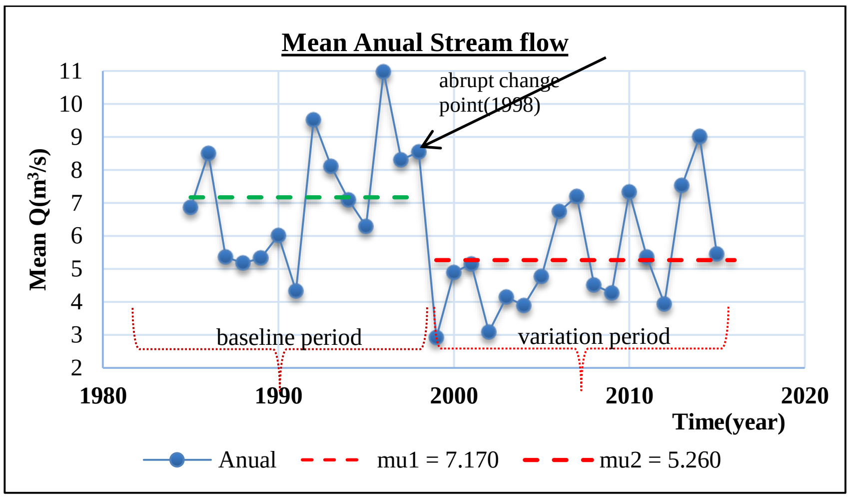

Figure 4.12. *Trends in mean annual stream flow over the study period (1985-2015)*
Note: -Green and red broken lines show the means in observed mean annual stream flow data.

4.3. Model Calibration, Validation, Sensitivity Analysis and Uncertainty Analysis

4.3.1. Sensitivity analysis results

After an initial SWAT simulation was conducted, a sensitivity analysis was performed to highlight basin specific parameters that drive model simulations and create sensitivities to model outputs (Arnold *et al*., 2012). SWAT-CUP 5.1.6.2 is an interface developed for SWAT that can do sensitivity analysis, calibration, validation, uncertainty analysis as well as easily be linked to SWAT. It was designed as an interface for SWAT to link the inputs and outputs of a calibration program to the model through text file formats. Highlighting sensitive parameters was necessary for calibration to assess over and underestimation of output variables, a sensitivity analysis was conducted using SWAT-CUP and a chosen algorithm was the Sequential Uncertainty Fitting version.2 (SUFI-2).

Eighteen stream flow parameters were observed for sensitivity analysis of stream flow using the automated Latin Hypercube One factor at a time (LH-OAT) sensitivity analysis provided in SWAT-CUP. Parameters chosen for calibration manipulation were listed in Table 4.12. Using the LH-OAT analysis, a t-test was produced to identify the significance and sensitivity of each parameter. Srinivasan (2015) recommended that without expert knowledge, a trial and error method of parameter range adjustment be used for calibration using SWAT-CUP.

Table 4.12. *Summary of sensitivity analysis on the 18 input parameters*

№	Parameter name	Description	Fitted Value	Min value	Max value
1	r__CANMX.hru	Maximum canopy storage	3.01	1.31	7.92
2	r__SOL_Z(..).sol	Depth from soil surface to bottom of layer	0.15	0.07	0.20
3	r__SOL_AWC(..).sol	Available water capacity of the soil layer	0.84	0.38	0.98
4	r__SOL_K(..).sol	Saturated hydraulic conductivity	13.01	6.24	18.43
5	v__CH_K2.rte	Effective hydraulic conductivity in main channel alluvium	298.16	154.41	327.81
6	r__CN2.mgt	SCS runoff curve number	-0.22	-0.23	-0.11
7	v__ESCO.hru	Soil evaporation compensation factor	0.53	0.07	0.77
8	a__GWQMN.gw	Threshold depth of water in the shallow aquifer required for return flow to occur (mm)	3419.45	1728.99	3979.93
9	v__ALPHA_BF.gw	Base flow alpha factor (days)	0.12	0.11	0.59
10	r__RCHRG_DP.gw	Deep aquifer percolation fraction	0.35	0.06	0.90
11	v__GW_REVAP.gw	Groundwater "revap" coefficient	0.12	0.09	0.14
12	v__REVAPMN.gw	Threshold depth of water in the shallow aquifer for "revap" to occur (mm)	55.50	46.91	390.46
13	v__GW_DELAY.gw	Groundwater delay (days)	434.53	223.83	447.27
14	r__OV_N.hru	Manning's "n" value for overland flow	18.61	3.11	19.91
15	r__SOL_BD(..).sol	Moist bulk density	1.48	0.99	1.88
16	r__SLSUBBSN.hru	Average slope length	36.54	28.94	39.14
17	r__HRU_SLP.hru	Average slope steepness	0.82	0.32	0.84
18	r__EPCO.hru	Plant uptake compensation factor	0.49	0.35	0.82

In SUFI-2, the assessment of the sensitive parameters is measured using the t-stat values where the values are more sensitive for a larger in absolute t-stat values. P-values are used to determine the significance of the sensitivity where the parameter becomes significance if the P-values are close to zero (Khalid *et al*., 2016). Based on p-value and t-value from eighteen parameters ten parameters were selected as the most sensitive parameters. The parameters the absolute value of t-value is high and p-value close to zero that parameter is the most sensitive parameter the result was described in the Table 4.13.

Table 4.13. *The most sensitive parameters*

№	Parameters name	t-Stat	P-Value	Rank
1	v__ALPHA_BF.gw	-20.72	0.00	1
2	r__SOL_K(..).sol	-12.88	0.00	2
3	r__HRU_SLP.hru	-2.51	0.01	3
4	v__GW_DELAY.gw	-2.11	0.04	4
5	r__CN2.mgt	-1.57	0.12	5
6	r__SLSUBBSN.hru	-1.40	0.16	6
7	v__ESCO.hru	-1.16	0.25	7
8	a__GWQMN.gw	-0.91	0.36	8
9	v__GW_REVAP.gw	-0.70	0.48	9
10	r__CANMX.hru	-0.49	0.62	10

4.3.2. Calibration and validation results

Calibration included observed stream flow measurements from the Aposto station for the years of 2006 to 2010, whereas validation used years 2011 to 2015. Final simulated stream flow statistics for the upper Gidabo watershed were NSE 0.90, R^2 0.91 and NSE 0.73, R^2 0.75 for calibration and validation respectively. Both calibration and validation included all eighteen parameter inputs. Visual representation of simulated outputs for calibration and validation were represented in Figure 4.13. Simulations used observed stream flow measurements from the Aposto River gauging station. The calibration and validation figures showed that the model did reproduce historical data very well.

Table 4.14. *The objective functions value and methods*

Method		Objective function values				
		p-factor	r-factor	R^2	NSE	PBIAS (%)
SUFI-2	Calibration	0.93	1.45	0.91	0.90	5.0
	Validation	0.88	1.26	0.75	0.73	12.4

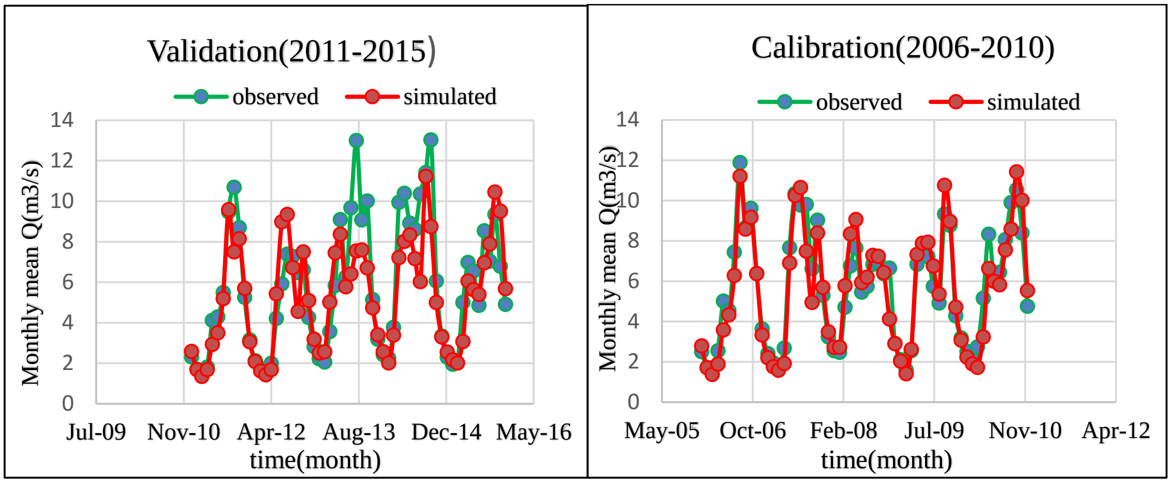

Figure 4.13. *The result of calibration and validation for average monthly stream flows*

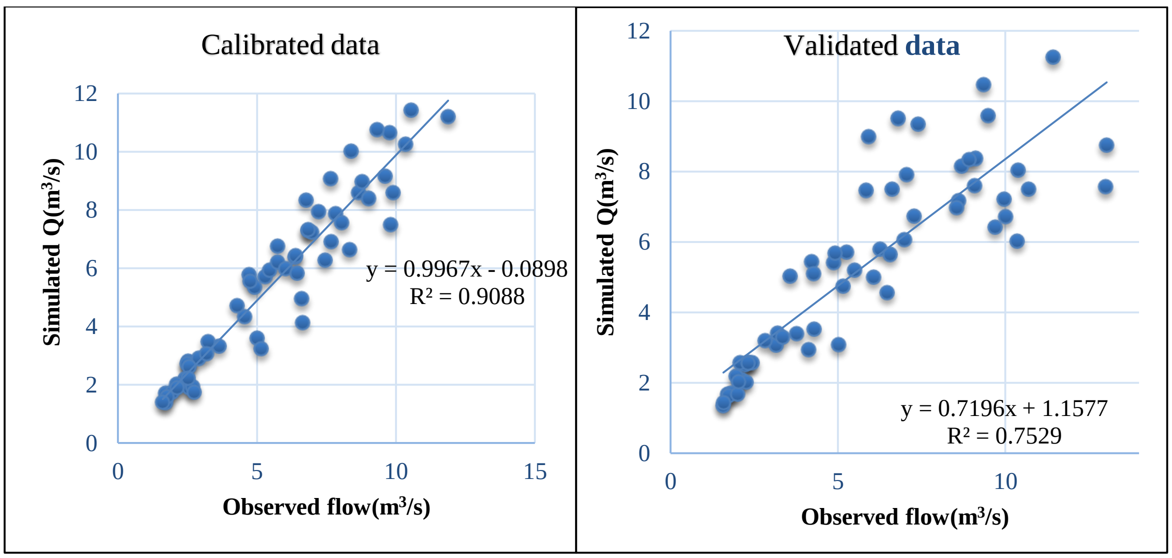

Figure 4.14. *Scatter plots of the calibration and validation periods*

4.3.3. Uncertainty analysis results

All sources of uncertainty were mapped to a set of parameter ranges. Two different indices were used to quantify the goodness of calibration uncertainty performance. The percentage of data bracketed by the 95% prediction uncertainty (95PPU) band (P-factor) and a measure of the average width of the 95PPU (R-factor), Abbaspour (2015) suggested for P-factor, a value of >70% and R-factor of around 1.

For this study, the P-factor and R-factor were described in Table 4.14. The result showed that the observed flow was bracketed in the 95PPU suggesting very good results or a minimal uncertainty in the model, which indicates SUFI-2 was able to capture most uncertainties.

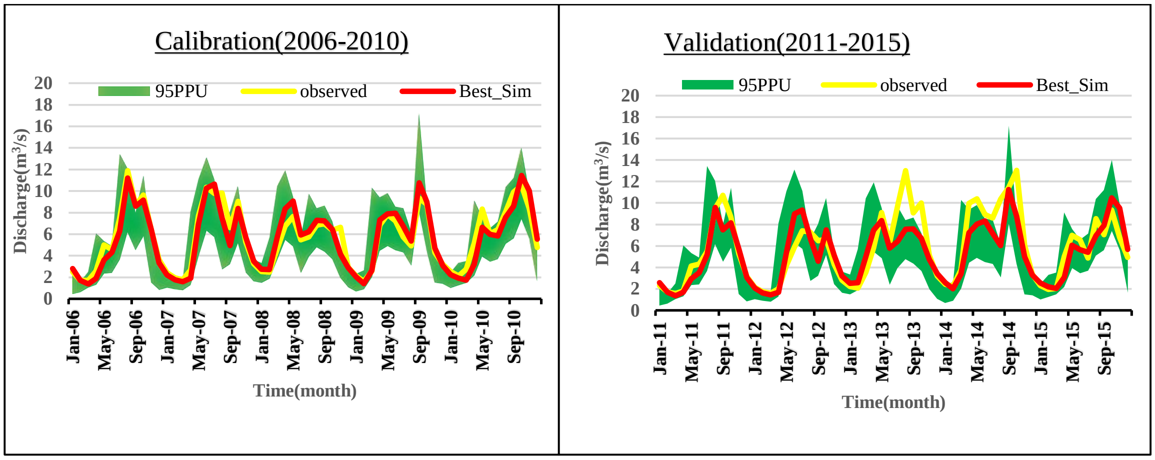

Figure 4.15. *95PPU analysis results*

4.4. Results of Simulated Stream Flow Components

The results of annual stream flow components simulated by SWAT under different scenarios were shown in Table 4.15. For baseline period scenario (S1) by using LULC map of 1985 and climate (1985-1998) the mean annual simulated stream flow component such as surface runoff, lateral flow and base flow values were 128.33mm/year, 49.96mm/year and 445.35mm/year respectively. For the second scenario(S2) by using LULC map of variation period (LULC map of 2016) holding climate constant that means climate of 1985-1998, the simulated mean annual surface runoff, lateral flow and base flow values were 167.02mm/year, 43.91mm/year and 417.81mm/year respectively.

Under scenario three(S3) using LULC map of baseline period, that island use and the cover map of 1985 and climate of variation period that means changing climate by holding LULC constant, that is the climate of (1999-2016). Thus, the simulated results of surface runoff, lateral flow and base flow were 99.36mm/year, 49.02mm/year and 376.03mm/year respectively. Finally, under variation scenario (S4) the LULC map (LULC map 2016) and climate (1999-2016) of variation period were used. The results of surface runoff, lateral flow and base flow were 137.24mm/year, 42.79mm/year and 350.61mm/year respectively.

Table 4.15. *Simulated values of mean annual stream flow components*

Scenarios	LULC	Climate	Mean annual simulated values (mm/year)		
			Surface runoff	Lateral flow	Base flow
Baseline period	*L1*	*C1*	128.33	49.96	445.35
LULC change only	*L2*	*C1*	167.02	43.91	417.81
Climate change only	*L1*	*C2*	99.36	49.02	376.03
LULC and Climate change	*L2*	*C2*	137.24	42.79	350.61

Note: - *L1* is land use map of baseline period that is land use map of 1985

L2 is the land use map of variation period that is land use map 2016

C1 is climate of baseline period (1985-1998)

C2 is climate of variation period (1999-2016)

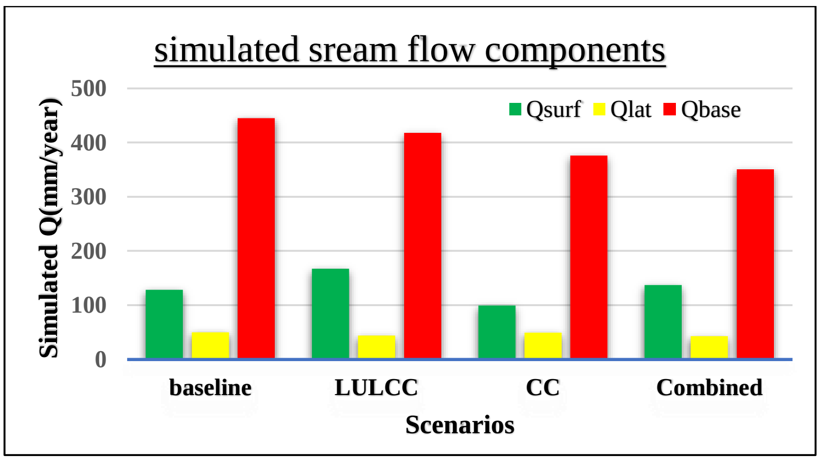

Figure 4.16. *Simulated stream flow components in different scenarios*

4.5. Contribution of LULC and Climate Change on Stream Flow Reduction

The effect of LULCC and climate change on stream flow components were calculated by measuring the difference between scenarios. Four different scenarios were simulated and compared against the baseline period in order to study the effects of LULCC and climate change on stream flow components.

Table 4.16. *Change in stream flow components due to LULCC and climate change.*

Scenarios	Change in stream flow components (mm/year)		
	ΔQ_{surf}	ΔQ_{lat}	ΔQ_{base}
Baseline period	0	0	0
ΔQ_{LULCC}	+38.29(56.5%)	-6.23(86.89%)	-26.48(27.95%)
$\Delta Cl_{imate\ change}$	-29.47(43.5%)	-0.94(13.11%)	-68.26(72.05%)
Combined	+8.82	-7.17	-94.74

Surface runoff: - LULCC contributed to an increase in surface runoff by 38.29mm/year during the entire period from 1985-2016. This change account 56.5% of the total change. At the same time, climate change contributed to a decrease in surface runoff by 29.47 mm/year in the watershed, this change account 43.5%. Both LULC and climate change contributed increase in surface runoff by 8.82mm/year during the entire study period in the watershed.

The increment of surface runoff was due to the conversion of forest land to agricultural land and built-up areas. The results of the LULC classification showed that from 1985-2016 the agricultural land was increased from 240.29km^2 in 1985 to 379.06km^2 in 2016 by the annual rate of change at 1.81%. The forest land (mixed forest and evergreen forest) was decreased; mixed forest from 236.76km^2 in 1985 to 140km^2 in 2016 and evergreen forest from 88.14km^2 in 1985 to 36.38km^2 in 2016. The built-up areas increased from 19.44km^2 in 1985 to 33.95km^2 in 2016.

Different studies support these results. For example, the study by Brook *et al*. (2011) in Anger watershed, in Ethiopia concluded that the surface runoff increased and the base flow decreased due to the expansion of agricultural land and declined of forest land.

The study by Zewude (2016) in Gidabo River Basin used different period of land cover (1973, 1986, 2000 and 2014) images. The result indicated that the mean annual flow for 2014 land cover was increased by 6.06% relative to that 1973 land cover period while the peak flow for 2000 land cover was also increased by 4.27% than the 1973 land cover. That indicated the increase in surface runoff and high flows could be explained by the increased area under agriculture. Moreover, base flow decreases as the surface runoff increase.

The study by Geremew (2013) shows that the expansion of agricultural lands over the forest that result in the increase of surface runoff following rainfall events. It can be explained in terms of the crop soil moisture demands. Crops need less soil moisture than forests; therefore, the rainfall satisfies the soil moisture deficit in agricultural lands more quickly than in forests thereby generating more surface runoff where the area under agricultural land is extensive. Moreover, this causes variation in soil moisture and groundwater storage. This expansion also results in the reduction of water infiltrating into the ground.

The surface runoff decreased due to climate change. The statistical MK results showed that annual rainfall trend in all stations within the watershed and around the watershed showed that decreasing trend and temperature trend in all stations shows statistically increasing trends in the watershed. Thus, a decrease in precipitation caused by climate change reduces water income in the catchment and the increasing temperature causes the increment of evapotranspiration and reduces surface runoff. This result was supported by the different studies. For example, the study by Yin *et al*. (2017) concluded that the influence of climate change on surface runoff agrees with climatic warming and drying trends. Decreasing precipitation will potentially lead to less runoff, whereas increasing temperatures will result in increased evaporation.

According to the study by Zhang *et al*. (2017), while rainfall decreased, the annual evapotranspiration and potential evapotranspiration increased by 4.4mm and 30.9mm, respectively, with the warmer air temperature. Climatic variables, especially rainfall, largely determine the runoff hydrograph of a basin. Reduced rainfall resulted in the significant decline of surface runoff by 61.8%.

The surface runoff was increased due to LULCC and was decreased due to climate change. On the other hand, due to the combined impact of LULCC and climate change, contributed to the increase in surface runoff because LULC change has the dominant impact on the increase in surface runoff in the entire study period in the watershed. Thus, in upper Gidabo watershed from 1985 to 2016, the impact of climate change on surface runoff is more significant than LULCC.

Lateral flow: - was decreased due to LULCC by 6.23mm/year accounts (86.89%) and due to climate change, 0.94mm/year accounts (13.11%) and due to combined impact it was decreased by 7.17mm/year, thus the dominant impact contributed from LULCC, which is (86.89%). The study by Takala *et al*. (2016) in Gilgel Gibe Omo Gibe River Basin showed that from 2001 to 2010 surface runoff was increased while lateral flow and total aquifer recharge has decreased. This attributed by the expansion of agricultural was directly land over forest causing the variation of soil moisture condition and groundwater storage. Change in forest/rangeland cover results in the reduction of water infiltrating into the ground, changing the infiltration rate, affecting the retention capacity of soils, contributing flow to runoff, and increasing the rate of sediment yields. These result revealed that the land use land cover change have significant effects on infiltration rates, on runoff production, water yield, sediment loading, evapotranspiration and water retention capacity of the soil.

Temperature, next to rainfall plays a significant role in the loss of water over a watershed. The rise in temperature increases the loss of soil moisture both directly and through transpiration. So the runoff amount, which flows toward the stream, was determined by soil moisture status (Belihu *et al*., 2018).

Base flow: - In the watershed, base flow was decreased due to LULCC by 26.48mm/year and accounts 27.95%. It also was decreased due to climate change during the entire period by 68.28mm/year this accounts 72.05% of the combined impact. The base flow was affected by the combined effect of LULCC and climate change by 94.74mm/year.

In general, base flow decreased by the combined impact of LULCC and climate change during the study period in the catchment by the rate of 94.74mm/year. Thus, the dominant factor that influenced base flow in the entire watershed during the study period is climate change.

This study result agreed with the study by Mechal *et al*. (2015) in Gidabo River Basin, which revealed that a drop in recharge due to a decrease in precipitation would have significant impact on a river base flow and under high or low warming trends a very slight proportional change in evapotranspiration results in a high relative change in recharge and surface runoff.

The study by Zewude (2016) in Gidabo River Basin showed that the increase in surface runoff and high flows could be explained by the increased area under agriculture. Moreover, base flow decreases as the surface runoff increase. From both studies, LULCC decreases base flow and the decreasing rainfall also reduces recharge to the groundwater.

Ghaffari *et al*. (2010) showed that decreasing grassland and increasing agricultural land decreased groundwater recharge and base flow in the semi-arid Zanjanrood Basin in Iran.

According to the study by Zhang *et al*. (2017) With a decline in precipitation and an increase in water loss by evapotranspiration, there would be less soil water percolating past the root zone to groundwater, resulting in declines in percolation, groundwater flow and water yield reduced by 72.2%, 72.1% and 39.3% respectively.

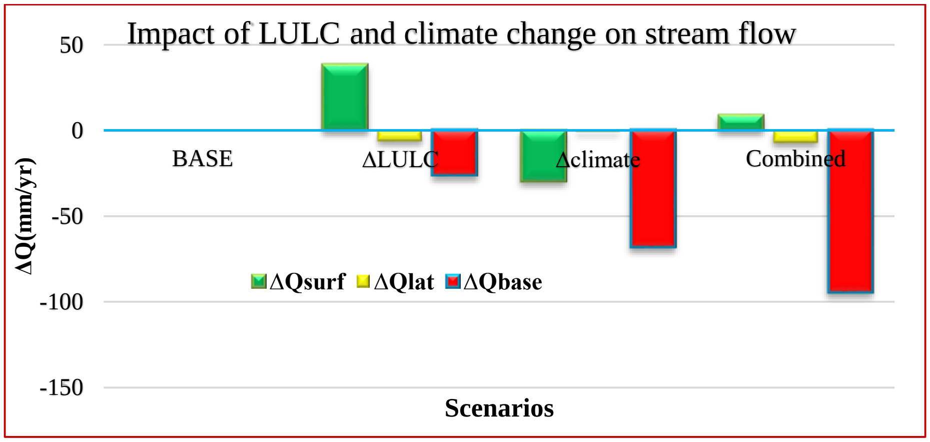

Figure 4.17. *Change in stream flow due to LULCC, Climate change and combined change*

Note: - ΔQL, ΔQC and Combined are change in surface runoff due to land use/cover change, climate change and both respectively.

4.6. Average Annual Water Balance Components of the Watershed

The SWAT model estimated other relevant water balance components in addition to monthly discharge. Average annual basin values for different water balance components during a base simulation periods presented in Table 4.16 shows average annual watershed gain and losses with land use and land cover change. From these components total water yield is the amount of stream flow leaving the outlet of watershed during the time step. The total water yield mathematically can be expressed as surface runoff plus lateral soil flow contribution to stream flow plus ground water contribution to stream flow minus water lost from tributary channels in the HRU via transmission through the bed.

Table 4.17. *Water balance due to land use and cover change*

Year	Rainfall(mm)	ET(mm)	$Q_{surf(mm)}$	$Q_{lat(mm)}$	$Q_{base(mm)}$	Water yield(mm)
1985	1137.6	556.9	108.76	42.27	381.53	532.56
2002	1137.6	553.5	132.65	40.49	368.53	541.67
2016	1137.6	552.5	146.3	41.15	355.86	543.31

CHAPTER FIVE

5. CONCLUSION AND RECOMMENDATIONS

5.1. Conclusion

This study examined separate and combined impacts of climate change and LULC change for the past 32 years, on stream flow reduction in the upper Gidabo watershed in Southern Ethiopia. Four scenarios were established using the hydrological modeling approach and one factor at a time (OFAT) experiment, and the SWAT model simulated the stream flow components (surface runoff, lateral flow and base flow) during past periods under each scenario. The simulated results for each scenario were compared with those for the baseline period.

LULC showed an increasing variation in agricultural land and built-up with the magnitude of change 138.78km^2 and 14.52km^2 by the annual rate of change by 1.81% and 2.33% respectively. Areas under mixed forest, evergreen forest and grazing lands showed decreasing trends by 96.58km^2, 51.77km^2 and 4.86km^2 by the annual rate of change 1.27%, 1.84% and 0.30% respectively of the entire watershed area. The MK test result showed that the mean annual maximum and minimum temperature was rising significantly while annual precipitation was decreasing and observed mean annual stream flow was decreasing during the period of 1985 to 2016.

The SWAT model was used to simulate the effects of LULC and climate changes on stream flow reduction in upper Gidabo watershed. The satisfactory performance of the SWAT model was confirmed by the Nash-Sutcliffe coefficient and coefficient of determination values of monthly runoff of 0.90 and 0.91 respectively during the calibration period, and 0.73 and 0.75, respectively, during the validation period.

The scenarios comparison effect showed that the combined effects of LULCC and climate changes contributed increase in surface runoff, decrease in lateral flow and base flow by 8.82mm/year, 7.17mm/year and94.74mm/year from 1985 to 2016. The isolated results indicated that the LULCC contributed to an increase in surface runoff by 38.29mm/year this accounts 56.5%, lateral flow decreased by 6.23mm/year accounts86.89% and base flow decreased by 26.48mm/year this accounts 27.95% while the climate change contributed to a reduction in surface runoff, lateral flow and base flow by 29.47mm/year (43.5%), 0.94mm/year (13.11%), and 68.26mm/year (72.05%) respectively.

In general, results showed that the climate change had the higher impact on base flow reduction than LULCC and LULCC had high impact on surface runoff and lateral flow reduction during the entire study period in the study watershed.

5.2. Recommendations

This study indicated the contributions of LULCC and climate change to watershed stream flow reduction. This suggested that the level of priority on LULC management and climate change adaptation should be made for the watershed. For instance, the forest region of the watershed should be strictly protected because of its critical role in protecting hydrologic function. It is urgent to control the rate and scale of expansion of agricultural lands because of its negative effect on the hydrological cycle.

To mitigate the negative impacts of climate change combined with LULC change, local policymakers are encouraged to apply science-based land use planning and implement adaptive integrated watershed management (AIWM) approaches. To address the water shortage problem, less productive croplands and some high water consumption cropping systems should be transformed into low water consumption ones with agroforestry supported agricultural practices. Efficient water allocation shall emphasis on providing equal attention with equity principles to ecological, agricultural, industrial and human consumption functions.

Future agriculture policy should further support studies related to climate-smart agriculture for coping with climate change. Availability of inadequate good quantity and quality data was a great challenge in the study area. Hence, it is highly recommended to establish good gauging networks of both hydrological and meteorological stations.

REFERENCES

Abbaspour, K.C. (2015). User manual for SWAT-CUP, SWAT calibration and uncertainty analysis programs. Swiss federal institute of aquatic science and technology, Eawag, Duebendorf, Switzerland.

Ahn, K.H. and Merwade, V. (2014). Quantifying the relative impact of climate and human activities on stream flow. *J. Hydrol*. 515, 257-266.

Anderson, J., Hardy, E., Roach, J. and Witmer, R. (1976). A land use and land cover classification system for use with remote sensor data. Geological survey professional paper 964.

Anzhou, Z., Xiufang, Z., Xianfeng, L., Yaozhong, P. and Depeng, Z. (2016). Impacts of land use change and climate variability on green and blue water resources in the Weihe River Basin of northwest China. *Catena* 137, 318-327.

Arnold, J., Moriasi, P., Gassman, K., Abbaspour, M., White, R., Srinivasan, C., Santhi, R., Harmel, A., Van Griensven and M. Van Liew. (2012). SWAT model use, calibration, and validation. *Transactions of the ASABE* 55(4), 1491-1508.

Arnold, J.G., Srinivasan, R., Muttiah, R.S. and Williams, J.R. (1998). Large area hydrologic modeling and assessment Part I: Model development. *J. Am. Water Resour. Assoc*. 34, 73-89.

Arnold, J.G., Williams, J.R and Maidment, D.R. (1995). Continuous time water and sediment routing model for large basins. *Journal of hydraulic engineering* 121(2), 171-183.

Ayana, A.B., Edossa, D.C and Kositsakulchai, E. (2014). Modeling the effects of land use changes and management practices on runoff and sediment yields in Fincha Watershed, Blue Nile, OIDA. *International journal of sustainable development 07:11.*

Baker, T. J., and MillerS. N. (2013). Using the soil and water assessment tool (SWAT) to assess land use impact on water resources in an East African watershed. *Journal of Hydrology*, 486,100-111.

Belete, M. (2013). The impact of sedimentation and climate variability on the hydrological status of Lake Hawassa, Southern Ethiopia. Doctoral dissertation. Friedrich Wilhelms Universität Bonn, Germany.

Belihu, M., Abate, B., Tekleab, S., and Bewket, W. (2018). Hydro-meteorological trends in the Gidabo catchment of the Rift Valley Lakes Basin of Ethiopia. *Physics and chemistry of the earth.* 104, 84-101.

Brook, H., Argaw, M., Sulaiman, H. and Abiye, T. A. (2011). The impact of land use/cover change on hydrology components due to resettlement activity: SWAT model approach. *International journal of ecology and environmental sciences* 37 (1), 49-60.

Budyko, M.I. (1974). Climate and life. Academic press, New York, CA.

Caetano, M., Mata, F. and Freire, S. (2005). Accuracy assessment of the Portuguese CORINE land cover map.

Chien, H., Yeh, P. and Knouft, J. (2013). Modeling the potential impacts of climate change on stream flow in agricultural watersheds of the Midwestern United States. *Journal of hydrology*, 491, 73-88.

Cuo, L. (2016). Land use/cover change impacts on hydrology in large river basins. Terrestrial water cycle and climate change: natural and human induced impacts. *John Wiley and sons, Inc., 103-134.*

Dai, A., Trenberth, K.E. and Karl, T.R. (1998). Global variations in droughts and wet spells: 1900-1995. *Geophys. res. Lett*., 25(17), 3367-3370.

Danuso, F. (2002). Climak: a stochastic model for weather data generation. *Italian journal of agronomy 6 (1):* 57-7, 67-68.

Donizete, R., Mauro, A., Demetrius, D. and Fernando, F. (2016). Hydrological simulation in a basin of typical tropical climate and soil using the SWAT Model Part II: simulation of hydrological variables and soil use scenarios. *Journal of hydrology: Regional Studies* 5,149-163.

Dooge, J.C.I. (1992). Sensitivity of runoff to climate change. A Hortonian approach. Bull. *Am. Meteorol. Soc.* 73 (12), 2013-2024.

Driessen, T., Hurkmans, R., Terink, W., Hazenberg, P., Torfs, P. and Uijlenhoet, R. (2010). The hydrological response of the Ourthe catchment to climate change as modeled by the HBV model. *Hydrology and earth system sciences,* 14(4), 651-665.

Easton, Z.M., Fuka, D.R., White, E.D., Collick, A.S., Biruk, A.B., McCartney, M., Awulachew, S.B., Ahmed, A.A. and Steenhuis, T.S. (2010). A multi basin SWAT model analysis of runoff and sedimentation in the Blue Nile, Ethiopia. *Hydrology and earth system sciences discussions,* 7, 3837-3878.

Ficklin, L., Stewart, T. and Maurer, E. (2013). Effects of projected climate change on the hydrology in the Mono Lake Basin, California. *Climatic change*, 116 (1), 111-131.

Gao, G., Fu, B., Wang, S., Liang, W. and Jiang, X. (2016). Determining the hydrological responses to climate variability and land use/cover change in the Loess Plateau with the Budyko frame work. *Sci. total environ*. 557,331- 342.

Gao, P., Mu, X.M., Wang, F., Li, R. (2011). Changes in stream flow and sediment discharge and the response to human activities in the middle reaches of the Yellow River. *Hydrol. earth syst. Sci.* 15 (1), 1-10.

Geremew, A. (2013). Assessing the impacts of land use and land cover change on hydrology of watershed. A case study on Gilgel-Abbay watershed, Lake Tana Basin, Ethiopia. Msc thesis. University of Jaume.

Ghaffari, G., Keesstra, S., Ghodousi, J. and Ahmadi, H. (2010). SWAT simulated hydrological impact of land use change in the Zanjanrood Basin, Northwest Iran. *Hydrological processes,* 24(7), 892-903.

Golmar, G., Ramesh, R., Trevor, D., Pradeep, G. and Mari, V. (2017). Predicting the temporal variation of flow contributing areas using SWAT. *Journal of hydrology.* 547, 375-386.

Guo, H., Hu, Q. and Jiang, T. (2008). Annual and seasonal stream flow responses to climate and land-cover changes in the Poyang Lake Basin, China. *Journal of hydrology,* 355(1-4), 106-122.

Guo, J., Su, X., Singh, V., Jin, J. (2016). Impacts of climate and land use/cover change on stream flow using SWAT and a separation method for the Xiying River Basin in Northwestern China. *Water* 8 (5), 192.

Gupta, V., Sorooshian, S. and Yapo, P. (1999). Status of automatic calibration for hydrologic models: comparison with multilevel expert calibration. *Journal of hydrology engineering*, 4, 135-143.

Hamed, H. and Rao, R. (1998). A modified Mann-Kendall trend test for auto-correlated data. *Journal of hydrology*, 204(1-4), 182-196.

Han, E., Merwade, V., Heathman, G.C. (2012). Implementation of surface soil moisture data assimilation with watershed scale distributed hydrological model. *J. Hydrol. 416-417, 98-117*.

Hanson, R. L. (1988). Evapotranspiration and droughts. Paulson, RW, Chase, EB, Roberts, RS and Moody, DW, Compilers, National Water Summary: 99-104.

Hu, Z., Wang, L., Wang, Z., Hong, Y., Zheng, H. (2015). Quantitative assessment of climate and human impacts on surface water resources in a typical semi-arid watershed in the middle reaches of the Yellow River from 1985 to 2006. *International journal of climatology*.35, 97-113.

Huntington, T.G. (2006). Evidence for intensification of the global water cycle: Review and synthesis. *Journal of hydrology,* 319(1-4), 83-95.

IPCC (Intergovernmental Panel on Climate Change). (2007). Climate change 2007: the fourth IPCC scientific assessment. In: M.L. Parry, O.F. Canziani, J.P. Palutikof, P.J. vander Linden and C.E. Hanson (eds). Intergovernmental panel on climate change. Cambridge University Press, Cambridge, United Kingdom and New York, NY, USA.

IPCC (Intergovernmental panel on climate change). (2014). Climate change. Synthesis Report. Contribution of working groups I, II and III to the fifth assessment report of the intergovernmental panel on climate change. Geneva, Switzerland, pp. 151.

Jackson, B., Carpenter, R., Dahm, N., McKnight, M., Naiman, J., Postel, L. and Running, W. (2001). Issues in Ecology: Water in a changing world. *Ecological applications,* 11(4), 1027-1045.

Jha, K. (2011). Evaluating hydrologic response of an agricultural watershed for watershed analysis. Water 3, 604-617.

Jha, K. and Gassman, P. (2014). Changes in hydrology and stream flow as predicted by a modeling experiment forced with climate models. *Hydrological processes,* 28(5), 2772-2781.

Jianyun. Z. and Lirong, S. (2012). Hydrological response to climate change in Beijiang River Basin based on the SWAT Model. *Procedia engineering,* 28(0), 241-245.

Jothityangkoon, C., Sivapalan, M., Farmer, DL. (2001). Process controls of water balance variability in a large semi-arid catchment: downward approach to hydrological model development. *Journal of hydrology*, 254, 174-198.

Kannan, N., White, S.M., Worrall, F., Whelan, M.J. (2007). Hydrological modeling of a small catchment usingSWAT-2000 ensuring correct flow partitioning for contaminant modeling. *J. Hydrol* 334, 64-72.

Kedir, Y. (2002)**.** Hydrogeology of upper Gidabo River catchment, Southern Ethiopia. Unpublished Msc Thesis Addis Ababa University, Ethiopia.

Kendall, M.G. (1975). Rank correlation methods, fourth ed. Charles Griffin, 212 pp.

Khalid, K., Ali, M., Rahman, N., Mispan, M., Haron, S., Othman, Z. and Bachok, M. (2016). Sensitivity analysis in watershed model using SUFI-2 algorithm. *Procedia engineering*162, 441-447.

Kindu, M., Schneider, T., Teketay, D. and Knoke, T. (2015). Drivers of land use/land cover changes in Munessa Shashemene landscape of the South-Central highlands of Ethiopia. *Environmental monitoring and assessment*187:452.

Kong, D., Miao, C., Wu, J., Duan, Q. (2016). Impact assessment of climate change and human activities on net runoff in the Yellow River Basin from 1951 to 2012. *Ecol. Eng.* 91, 566-573.

Kumar, S. and Neupane, R. P. (2015). Estimating the effects of potential climate and land use changes on hydrologic processes of a large agriculture dominated watershed. *Journal of hydrology*. 529, 418-429.

Kundu, S., Khare, D. and Mondal, A. (2017). Individual and combined impacts of future climate and land use changes on the water balance. *Ecol. Eng.* 105, 42-57.

Legesse, D., Vallet-Coulomb, C. and Gasse, F. (2003). Hydrological response of a catchment to climate and land use changes in tropical Africa: Case study south central Ethiopia. *Journal of hydrology*, 275, 67-85.

Li, J., Zhang, L., Wang, H., Wang, J., Yang, W., Jiang, J. (2007). Assessing the impact of climate variability and human activities on stream flow from the Wuding River Basin in China. *Hydrol. Process*. 21, 3485-3491.

Li, Z., Liu, Z., Zhang, C., Zheng, L. (2009). Impacts of land use change and climate variability on hydrology in the agricultural catchment on the Loess Plateau of China. *J. Hydrol*. 377 (1-2), 35-42.

Liang, W., Bai, D., Wang, Y., Fu, J., Yan, P., Wang, S., Yang, T., Long, D. and Feng, Q. (2015). Quantifying the impacts of climate change and ecological restoration on stream flow changes based on a Budyko hydrological model in China's Loess plateau. *Water Resour. Res*. 51 (8), 6500-6519.

Luo, K., Tao, F., Moiwo, P. and Xiao, D. (2016). Attribution of hydrological change in the Heihe River Basin to climate and land use change in the past three decades. Sci. Rep. 6.

Mamo, K. and Jain, M. (2013). Runoff and sediment modeling using SWAT in Gumera catchment, Ethiopia. *Open journal of modern hydrology*, 3,196-205.

Manandhar, R., Odeh, I. and Ancev, T. (2009). Improving the accuracy of land use and land cover classification of landsat data using post-classification enhancement.

Manish, K. and Rawat, J. S. (2015). Monitoring land use/cover change using remote sensing and GIS techniques. a case study of Hawalbagh block, district Almora, Uttarakhand, India. National authority for remote sensing and space sciences: *The Egyptian journal of remote sensing and space sciences, 18, 77-84.*

Mann, H.B. (1945). Non-Parametric tests against trend. Econometrica 13, 245-259.

Mechal, A., Wagner, T. and Birk, S. (2015). Recharge variability and sensitivity to climate: the example of Gidabo River Basin, main Ethiopian rift. *J. Hydrology Regional Stud*. 4, 644-660.

Melese, S. (2016). Effect of climate change on water resources. *Journal of water resources and ocean science.* 5(1), 14-21.

Meyer, W.B. and Turner, B. L. (1994). Changes in land use and land cover: A global perspective. Cambridge: *Cambridge University Press*. New York.

Miao, Y., Ni, R., Borthwick, L. and Yang, L. (2011). A preliminary estimate of human and natural contributions to the changes in water discharge and sediment load in the Yellow River. *Glob. planet. change*. 76 (3-4), 196-205.

Moriasi, D., Arnold, J., Vanliew, M., Bingner, R., Harmel, R., and Veith, T. (2007). Model evaluation guidelines for systematic quantification of accuracy in watershed simulations. *American society of agricultural and biological engineers*, 50 (3): 885-890.

Musa, M. K. and Odera, P. A. (2015). Land use land cover changes and their effects on agricultural land: A case study of Kiambu County, Kenya: *Kabarak journal of research and innovation volume 3 number 1: 74-86.*

Mwangi, M., Julich, S., Patil, D., McDonald, M.A. and Feger, K. (2016). Relative contribution of land use change and climate variability on discharge of upper Mara River, Kenya. *Journal of hydrology: Regional Studies* 5, 244-260.

Natkhin, M., Dietrich, O., Schäfer, M.P. and Lischeid, G. (2015). The effects of climate and changing land use on the discharge regime of a small catchment in Tanzania. *Reg. Environ. Chang*. 15 (7), 1269-1280.

Neitsch, S., Arnold, J., Kiniry, R. and Williams, J. R. (2011). Soil and water assessment tool theoretical documentation version-2009. Texas water resources institute.

NMSA, (1996). Climatic and Agro climatic Resources of Ethiopia. Meteorological Research Report Series, 1:1, January. Addis Ababa, Ethiopia.

Oki, T. and Kanae, S. (2006). Global hydrological cycles and world water resources. *Science*, 313 (5790), 1068-1072.

Pai, N. and Saraswat, D. (2011). SWAT 2009 _LUC: A tool to activate the land use change module in SWAT 2009. *Transactions of the ASABE* 54(5), 1649-1658.

Schilling, E., Gassman, P., Kling, C., Campbell, T., Jha, M., Wolter, C. and Arnold, J. (2014). The potential for agricultural land use change to reduce flood risk in a large watershed. *Hydrological processes*, 28(8), 3314-3325.

Setyorini, A., Khare, D. and Pingale, S.M. (2017). Simulating the impact of land use/land cover change and climate variability on watershed hydrology in the upper Brantas Basin, Indonesia. Appl. Geomatics.

Shanka, AS. (2017). Evaluation of climate change impacts on runoff in the Gidabo River Basin: Southern Ethiopia. *Environ Pollut Climate Change* 1: 129.

Sharpley, A.N. and Williams, J.R., eds. (1990). EPIC-Erosion/Productivity Impact Calculator: 1. model documentation. U. S. department of agriculture technical bulletin No. 1768. 235.

Shi, P., Ma, X., Hou, Y., Li, Q., Zhang, Z., Qu, S., Chen, C., Cai, T. and Fang, X. (2013). Effects of land use and climate change on hydrological processes in the upstream of Huai River, China. *Water Resour. Manag*. 27(5), 1263-1278.

Shimaa, M. (2015). Hydrological modeling of the Simly dam watershed (Pakistan) using GIS and SWAT model. *Alexandria engineering journal*.54, 583-594.

Shrestha, R.P., Binhn. D. and Son N.T. (2015). Effect of runoff and sediment yield in Da River Basin of Hoahbinh Province, Northwest Vietnam. *Journal of metrological sciences*.12 (4), 1051-1064.

Smakhtin, V.U. (2001). Low flow hydrology: A review. *Journal of hydrology*, 240(3-4): 147-186.

Solomon, H. (2005). GIS-based surface runoff modeling and analysis of contributing factors. A case study of the Nam Chun watershed. Thailand. M.Sc. Thesis ITC, Netherlands.

Sorribas, M.V., Paiva, R.C.D., Melack, J.M., Bravo, J.M., Jones, C., Carvalho, L., Beighley, E., Forsberg, B. and Costa, M.H. (2016). Projections of climate change effects on discharge and inundation in the Amazon Basin. *Clim. Chang*, 136 (3-4), 555-570.

Srinivasan, R. (2015). Soil and Water Assessment Tool beginner SWAT training manual. Workshop at spatial science laboratory, Texas A and M University. January 26-28,2015.

Sunde, M.G., He, H.S., Hubbart, J.A. and Urban, M.A. (2017). Integrating downscaledCMIP5 data with a physically based hydrologic model to estimate potential climate change impacts on stream flow processes in a mixed use watershed. *Hydrol. Process*. 31 (9), 1790-1803.

Takala, W., Adugna, T. and Tamam, D. (2016). The effects of land use land cover change on hydrological process of Gilgel Gibe, Omo Gibe Basin, Ethiopia. *International journal of scientific and engineering research, volume 7, issue 8.*

Tao, F., Luo, K., Xiao, D. and Moiwo, J. (2016). Attribution of hydrological change in Heihe River Basin to climate and land use change in the past three decades. *Scientific Reports.*

Tesemma, Z.K., Mohamed, Y.A. and Steenhuis, T.S. (2010). Trends in rainfall and runoff in the Blue Nile Basin: 1964-2003. *Hydrol. Process*. 24 (25), 3747-3758.

Tharme, R.E. (2003). A global perspective on environmental flow assessment: emerging trends in the development and application of environmental flow methodologies for rivers. *River research and applications*, 19(5-6), 397-441.

Trang, T., Shrestha, S., Shrestha, M., Datta, A. and Kawasaki, A. (2017). Evaluating the impacts of climate and land use change on the hydrology and nutrient yield in a trans-boundary river basin: a case study in the 3s River Basin (Sekong, Sesan, and Srepok). *Sci. Total Environ*. 576,586-598.

Trenberth, K.E. (1998). Atmospheric moisture residence times and cycling: implications for rainfall rates and climate change. *Climatic Change*, 39, 667-694.

US Global Change Research Program, (2009). The essential principles of climate sciences. Available at: http://www.climate.noaa.gov/education/pdfs/ClimateLiteracy-8.5x11- March09FinalHR.

Valentina, K., Fred, H., Shaochun, H., Cornelia, H., Tobias, V., Hagen, K., and Zbigniew, W. (2014). Modeling climate and land change impacts with SWIM: lessons learnt from multiple applications. *Hydrological sciences journal*, 10,125-136.

Veldkamp, W.S.A. (2001). Modeling the spatial dynamics of regional land use. The CLUE-S model. *Environmental management*, Vol. 30 (3), 301-405.

Wagner, D., Bhallamudi, M., Narasimhan, B., Kumar, S., Fohrer, N. and Fiener, P. (2017). Comparing the effects of dynamic versus static representations of land use change in hydrologic impact assessments. *Environ. Model. Soft.*

Wang, X., (2014). Advances in separating effects of climate variability and human activity on stream discharge: an overview. Adv. *Water Resour*. 71, 209-218

Welde, K. and Gebremariam, B. (2017). Effect of land use land cover dynamics on hydrological response of watershed: case study of Tekeze Dam Watershed, Northern Ethiopia. *International soil and water conservation research 5, 1-16.*

Wu, Y., Liu, S., Sohl, T. and Young, C. (2013). Projecting the land cover change and its environmental impacts in the Cedar River Basin in the Midwestern United States. *Environmental research letters*, 8(2), 024-025.

Xu, C.Y. (2002). Hydrologic models. Uppsala university department of earth sciences hydrology.

Xu, X., (2007). Impact of human activities on the stream flow of Yellow River. *Advances in Water Science* 18, 648-655.

Yang, L., Feng, Q., Yin, Z., Wen, X., Si, J., Li, C. and Deo, R.C. (2017). Identifying separate impacts of climate and land use/cover change on hydrological processes in upper stream of Heihe river, Northwest China. *Hydrol. Process.* 31 (5), 1100-1112.

Ye, C., Zhang, Q., Liu, J., Li, X.H. and Xu, C.Y. (2013). Distinguishing the relative impacts of climate change and human activities on variation of stream flow in the Poyang lake Catchment. China. *J. Hydrol*. 494, 83-95.

Yesserie, A. (2009). Spatio-temporal land use/land cover changes analysis and monitoring in the Valencia Municipality, Spain. Msc. thesis, University of Nova.

Yesuf, H., Assen, M., Alamirew, T. and Melesse, A. (2015). Modeling of sediment yield in Maybar gauged watershed using SWAT, Northeast Ethiopia. *Catena 127,191-205.*

Yin, J., He, F., Xiong, Y.J. and Qiu, G.Y. (2017). Effects of land use/land cover and climate changes on surface runoff in a semi-humid and semi-arid transition zone in northwest China. *Hydrol. Earth Syst. Sci*. 21 (1), 183-196.

Zeng, S., Zhan, C., Sun, F., Du, H., Wang, F. (2015). Effects of climate change and human activities on surface runoff in the Luan River Basin. *Adv. Meteorol*. 2015, 1-12.

Zewude, K. (2016). Land use land covers change analysis and runoff estimation using arc SWAT model in Gidabo Watershed. Unpublished Msc. Thesis, Institute of Technology, Hawassa University, Hawassa.93pp.

Zhang, L., Karthikeyan, R., Bai, Z. and Srinivasan, R. (2017). Analysis of stream flow responses to climate variability and land use change in the Loess Plateau Region of China. *Catena* 154:1-11.

Zhang, L., Nan, Z. Yu, W. and Ge, Y. (2016). Hydrological responses to land use change scenarios under constant and changed climatic conditions. *Environmental Management,* 57 (2), 412-431.

Zhang, L., Nan, Z., Xu, Y. and Li, S. (2016). Hydrological impacts of land use change and climate variability in the headwater region of the Heihe River Basin, Northwest China. PLoS One 11 (6), e0158394.

Zhang, L., Nan, Z., Yu, W., Zhao, Y. and Xu, Y. (2018). Comparison of baseline period choices for separating climate and land use/land cover change impacts on watershed hydrology using distributed hydrological models. *Science of the Total Environment*, (622-623), 1016-1028.

Zhang, T., Zhang, X., Xia, D. and Liu, Y. (2014). Analysis of land use change dynamics and its impacts on hydrological processes in the Jialing River Basin. *Water,* 6(12), 3758-3782.

Zhang, Y.F., Guan, D.X., Jin, C.J., Wang, A.Z., Wu, J.B., Yuan, F.H. (2011). Analysis of impacts of climate variability and human activity on stream flow for a River Basin in northeast China. J. Hydrol. 410 (3-4), 239-247.

Zhao, G.J., Tian, P., Mu, X.M., Jiao, J.Y., Wang, F. and Gao, P. (2014). Quantifying the impact of climate variability and human activities on stream flow in the middle reaches of the Yellow River Basin. China. J. *Hydrol.* 519, 387-398.

Zhao, Y.F., Zou, X.Q., Gao, J.H., Xu, X.W.H., Wang, C.L., Tang, D.H., Wang, T., Wu, X.W. (2015). Quantifying the anthropogenic and climatic contributions to changes in water discharge and sediment load into the sea: A case study of the Yangtze River, China. *Sci. Total Environ*. 536, 803-812.

Zuo, D.P., Xu, Z.X., Wu, W., Zhao, J. and Zhao, F. (2014). Identification of stream flow response to climate change and human activities in the Wei River Basin, China. *Water Resour. Manag*. 28, 833-851.

APPENDICES

Appendix 1. *Mean monthly river discharge data (m^3/s) of Aposto river gauging station*

year	Jan	Feb	Mar	Apr	May	Jun	Jul	Aug	Sep	Oct	Nov	Dec
1985	2.13	1.66	1.88	5.48	16.94	7.69	7.07	7.75	14.39	11.16	3.53	2.63
1986	1.60	1.73	2.23	4.45	9.05	25.93	11.34	8.36	18.47	12.30	3.68	2.73
1987	1.97	1.93	2.99	4.89	13.75	10.38	4.99	4.38	7.02	11.92	0.00	0.09
1988	0.20	0.66	1.37	4.55	2.66	4.62	6.64	11.46	10.75	12.43	4.52	2.21
1989	2.59	2.30	1.97	4.95	4.01	5.85	5.76	3.60	11.67	12.42	4.61	4.25
1990	2.41	3.80	6.05	10.10	10.58	6.26	6.29	6.01	6.82	6.94	3.75	3.18
1991	3.19	3.44	3.75	4.60	4.65	3.37	4.82	4.35	10.36	5.46	2.11	1.77
1992	1.16	1.55	1.20	6.63	6.51	5.04	7.14	22.81	19.48	27.46	10.74	4.47
1993	2.92	4.31	2.33	5.57	16.32	16.56	7.74	5.45	9.31	16.47	7.54	2.70
1994	1.81	1.45	1.72	3.13	9.79	6.87	16.02	17.69	12.56	6.37	5.31	2.44
1995	1.64	1.67	1.85	9.51	9.07	4.23	4.76	6.53	16.95	12.47	3.84	2.94
1996	2.86	1.88	5.98	11.29	14.83	16.02	15.92	18.21	18.78	19.23	4.13	2.60
1997	2.12	1.53	1.55	5.38	8.08	5.80	10.12	12.95	8.16	21.41	16.76	5.83
1998	2.06	1.05	1.19	3.34	10.10	4.48	7.58	23.14	10.93	29.75	6.11	2.73
1999	2.17	1.74	1.91	1.91	3.67	2.47	2.47	3.07	3.95	6.83	2.99	1.89
2000	1.41	1.30	1.27	1.96	4.91	3.02	2.51	7.83	7.20	18.48	6.27	2.45
2001	2.24	1.81	1.90	2.77	5.63	8.36	3.93	8.81	9.92	9.83	4.14	2.48
2002	2.01	1.56	2.04	2.93	3.94	5.29	2.71	3.66	4.89	3.53	2.19	2.24
2003	1.84	1.47	1.71	4.02	2.99	2.40	3.01	6.55	4.84	11.31	6.68	2.94
2004	2.33	1.99	2.41	4.31	6.62	3.24	2.79	4.02	6.21	7.94	2.62	2.17
2005	1.77	1.37	1.72	2.84	10.53	6.76	5.56	6.01	8.78	6.27	3.67	2.02
2006	1.65	1.67	2.75	4.56	9.25	5.27	10.96	13.93	8.87	10.99	6.37	4.54
2007	3.04	2.53	2.29	4.96	9.96	10.62	7.16	16.72	11.62	10.91	4.08	2.51
2008	2.01	1.73	1.53	2.01	3.43	4.06	4.34	5.47	6.20	6.25	14.17	2.93
2009	2.36	2.22	2.39	5.36	7.69	5.08	2.71	3.60	5.03	8.23	2.99	3.51
2010	3.41	2.79	5.74	10.93	13.41	6.20	8.29	9.55	13.84	7.86	3.51	2.41
2011	2.07	1.74	1.79	1.94	5.32	5.07	5.80	9.37	13.90	9.24	4.82	3.24
2012	2.18	1.84	1.74	2.33	3.00	2.88	5.44	7.83	8.39	5.75	3.44	2.46
2013	1.95	1.57	2.12	4.22	9.84	6.74	12.96	18.44	10.58	13.31	5.55	2.98
2014	2.30	2.50	4.15	12.70	12.76	9.52	10.03	14.69	11.62	17.31	7.13	3.38
2015	2.06	1.73	2.03	6.95	7.92	7.47	4.34	10.12	6.20	8.23	4.08	4.16

Appendix 2. *Annual rainfall data (mm) of climatic stations*

Year	Climatic stations				
	Yirgalem	A/wondo	H/wita	Morocho	Aposto
1985	1202.15	1670.51	1329.70	1428.10	928.39
1986	1432.41	1836.29	1421.60	1880.50	1224.88
1987	1297.88	1477.60	1138.90	1858.00	1259.13
1988	1429.82	1501.30	1254.19	2153.30	1387.13
1989	1315.92	1377.80	1097.20	1843.90	1496.91
1990	1202.93	1348.80	961.90	1757.10	1266.73
1991	1232.70	1356.40	1017.90	1565.40	1372.90
1992	1291.00	1580.20	1343.60	1574.90	1149.40
1993	1281.80	1640.30	1107.00	1290.00	1109.20
1994	1234.00	1560.60	1066.70	1541.00	1146.90
1995	1120.70	1424.10	923.30	1490.50	1061.90
1996	1472.20	1649.20	1168.40	1861.90	1467.94
1997	1390.90	1965.99	654.10	1379.70	1359.50
1998	1654.60	1575.50	1265.30	1193.70	919.80
1999	1075.70	1237.60	818.90	947.20	675.00
2000	1071.70	1425.30	1003.80	974.70	872.40
2001	1573.90	1972.80	1291.90	1225.40	928.80
2002	997.20	1457.20	860.78	840.30	829.10
2003	852.50	1483.10	1029.00	1018.60	849.20
2004	832.80	1282.40	1027.90	1043.90	929.30
2005	1100.80	1818.10	1303.50	1289.90	1031.40
2006	1422.90	1848.90	1458.20	1220.90	1508.70
2007	1472.20	2022.90	1471.20	1303.30	1377.00
2008	1224.10	1462.80	930.20	1035.30	989.40
2009	1090.50	1405.60	866.70	764.30	1013.90
2010	1228.20	1863.00	1360.70	788.00	1326.80
2011	852.70	1378.30	1181.92	1079.67	1330.90
2012	1207.60	1218.30	899.18	1038.10	901.70
2013	996.74	1592.72	1190.02	1092.08	1245.00
2014	1458.22	1737.89	1388.70	1000.81	1175.04
2015	874.87	1168.38	946.97	713.60	1017.05
2016	1342.16	1333.90	1407.80	1198.70	1086.62

Appendix 3. *Mean monthly temperature data (mm) of climatic stations (1985-2016)*

Month	Climatic stations			
	Yirgalem		Haysawita	
	Mean max temp(c°)	Mean min temp(c°)	Mean max temp(c°)	Mean min temp(c°)
January	28.1	9.99	24.21	10.73
February	29.7	10.86	25.18	11.55
March	30.75	11.96	24.82	12.22
April	29.08	12.31	23.64	12.34
May	26.41	12.13	22.81	11.77
June	23.16	12.14	21.41	11.61
July	21.24	12.33	20.57	11.48
August	21.97	12.28	20.73	11.28
September	23.76	12.09	21.47	11.18
October	25.5	11.45	22.35	11.03
November	27.94	10.51	23.59	10.4
December	27.99	9.93	23.77	10.48

Appendix 4. *Accuracy assessment points for2016 LULC map*

LULC classes														
Agricultural Land			Mixed Forest			Evergreen Forest			Grazing Land			Built Up Areas		
x	**y**	**Altitude**	**x**	**y**	**Altitude**	**x**	**y**	**Altitude**	**x**	**y**	**Altitude**	**x**	**y**	**Altitude**
434504	740536	1775	453992	752035	2586	452851	751752	2517	454092	744307	3069	434542	745564	1766
435264	739914	1807	449251	752508	2164	452579	751244	2544	455255	745068	3146	434405	746060	1773
440130	743611	1810	446864	751860	1985	452524	748649	2672	452672	745017	3001	436757	746137	1766
440433	742319	1848	445368	750671	1867	447696	751389	2054	455366	745085	3155	437894	745692	1773
437404	741804	1786	445464	753610	1955	452143	749120	2556	452253	745804	2956	430780	745389	1759
439595	743440	1820	442701	752236	1887	452608	747540	2783	452476	747677	2709	445491	746911	1998
436041	742531	1773	440951	750916	1831	451243	746750	2941	454751	747754	2903	430742	745331	1767
433871	747170	1736	441441	753855	1858	449778	744824	2528	456683	745513	3042	438411	759624	1866
432284	748150	1723	444668	752070	1936	448700	744753	2589	455067	748429	2910	438887	759871	1886
434053	751699	1778	448053	751738	1965	448758	744465	2507	453596	749002	2709	453595	760269	2401
434152	753321	1783	440859	747072	1816	446401	745974	2079	455306	748027	1801	453950	760277	2425
432516	753733	1795	442646	746481	1842	445898	746261	2060	450423	749088	2588	443020	755523	1920
432232	752553	1697	445389	745057	1849	452220	749120	2592	450107	747856	2396	441192	749928	1837
431720	749722	1747	442483	748575	1854	453140	746879	2789	432404	741947	1783	445551	746884	2006
440111	752240	1786	439510	749473	1812	449534	748373	2566	431942	742075	1765	445348	746640	2028
440723	754658	1845	443965	747351	1956	448930	750557	2494	430779	741408	1752	437612	745877	1785
440666	751415	1785	442693	746510	1837	457210	753959	2946	431292	740159	1772	445104	749964	1920
442458	754018	1809	439491	749464	1858	451246	753470	2421	430924	738817	1799	440783	748530	1733
442615	750391	1791	440495	747791	1811	450887	753566	2351	432524	743580	1749	441607	748419	1767
438647	755539	1836	439948	741927	1857	455155	751126	2729	435346	742845	1763	438760	747077	1778
445015	759772	1980	439272	742912	1844									
448149	757290	2078	442745	741755	1870									
445968	752176	1954	441407	739929	1901									
452475	756954	2555	440861	738886	1838									
448050	754056	2032	439250	740633	1842									
439865	759815	1853	443536	739346	2071									
448028	760857	2112	441975	737844	2073									
444375	764131	1999	439365	740906	1865									
439692	763786	1920	446678	739627	2515									
447369	761790	2106	443723	740382	2044									
437604	758287	1841	441465	740755	1897									
437368	762225	1903	439243	742934	1864									
436352	763804	1875	444873	742646	2050									
451834	759357	2330	441774	741827	1900									
443884	756871	1946	439222	742905	1871									
441507	759847	1887	441206	742503	1876									
456390	757197	2689	441673	743630	1860									
453468	757034	2577	439742	743797	1819									
438675	759557	1868	440837	743451	1816									
446643	755001	1998	438981	744109	1810									

Appendix 5. *Accuracy assessment points for 2002 LULC map*

LULC Classes									
Agricultural Land		Mixed Forest		Evergreen Forest		Grazing Land		Built Up Area	
x	**y**	**x**	**y**	**x**	**y**	**x**	**y**	**x**	**y**
433292.54	743952.16	445512.4	753968.12	449488.37	744749.83	450244.79	752697.93	434171.62	745797.83
434353.04	742709.86	444284.5	753340.84	448772.84	744587.21	451624.81	754463.54	434232.5	746081.95
436686.13	743830.96	445338.9	755583.05	446366.06	745985.74	453248.37	756553.87	434618.09	746061.65
433822.79	741331.22	441722	753914.74	445851.65	746311.31	454364.56	753651.77	436911.36	746122.54
432277.49	745542.9	446953.8	756477.27	445190.88	745612.78	456495.47	752028.21	431161.31	746220.61
436852.78	741922.07	450717.6	756864.32	444095.88	750011.63	455399.57	748618.75	430818.91	745408.63
437928.42	741937.22	447594.5	753153.99	447192.07	751333.18	457429.02	749410.23	430593.91	745124.93
441609.86	739876.82	449342.9	751272.13	449608.61	751446.45	457165.19	756777.11	435250.54	749341.34
445730.64	743755.21	451077.9	756624.08	451024.55	750710.16	440625.24	753570.59	432785.26	753469.71
441322.01	739816.22	447541.1	755756.56	451515.41	750106.03	438676.98	757893.3	438488.67	759613.34
437307.28	741331.22	447340.9	755409.55	452704.8	751219.9	435957.52	759699.5	438518.02	760024.22
435322.63	739876.82	445739.3	756917.71	450684.73	752163.86	433745.43	758339.78	434330.96	759975.31
436474.03	739285.98	448101.6	755943.41	452912.47	751805.16	433298.96	757609.18	434820.1	758468.75
433413.74	744043.06	449983.5	753394.22	454177.38	751975.07	435470.46	752596.46	444387.73	760161.18
432095.7	742588.66	449329.5	751232.09	444095.88	749992.75	431959.52	749369.64	445268.19	756903.49
429686.85	740800.97	452999.8	752913.75	448938.4	759392.75	432081.29	748070.8	438518.02	760170.96
432413.84	739225.38	454347.8	752446.62	445056.4	755014.88	432020.41	744884.58	438879.98	759681.82
432822.89	741482.72	457177.3	750284.49	453142.1	749605.28	432446.59	741901.3	439046.29	760190.53
434050.04	744649.06	439154.6	754262.1	443625.45	758075.14	431086.86	738816.55	438860.42	760836.2
437822.37	744800.56	457444.2	751405.59	444022.15	759633.6	434232.5	742692.78	441990.93	763066.69
435080.23	748194.14	456256.4	750845.04						
440519.06	747194.25	449329.5	751245.43						
446048.79	744012.76	458151.6	756410.54						
439549.47	749845.49	456843.6	752820.32						
444124.75	748951.64	457484.2	751378.9						
438549.57	746042.85	457284	750177.71						
434353.04	749618.24	444284.5	753380.88						
432580.49	749936.39	444911.8	754662.14						
433307.69	748800.14	448328.5	752406.58						
439140.42	754178.37	454267.7	752326.5						
439867.62	752451.28	456162.9	753394.22						
435413.53	753935.97	457217.3	752593.43						
445047.87	752497.41	444244.5	748562.78						
443770.93	753334.98	445018.6	752473.31						
434292.44	752587.63	445552.4	753340.84						
437382.98	761866.22	447314.2	750805						
438639.49	757347.62	448261.8	748816.37						
439207.33	759220.3	448502	751579.1						
448232.45	759268.63	446179.7	749763.97						
446408.09	761237.96	448422	753807.97						

Appendix 6. *Accuracy assessment points for 1985 LULC map*

LULC classes

Agricultural		Mixed Forest		Evergreen Forest		Grazing Land		Built Up Area	
x	**y**	**x**	**y**	**x**	**y**	**x**	**y**	**x**	**y**
435785.72	748740.1	440498.82	753834.85	452691.29	751429.64	432391.97	744331.29	434551	745839.51
437570.83	748219.78	443507.69	754735.15	457677.39	755058.27	431128.06	738914.55	438423.05	759633.71
439668.13	749860.8	450473.11	752816.1	450211.3	747618.28	435145.48	751734.18	437120.71	745982.25
436290.24	748881.59	456538.24	751560.43	445982.25	755084.37	435355.53	752525.89	435615.64	749472.99
436232.64	747143.84	441920.34	756156.66	449898.03	751429.64	431854.34	749288.23	432972.29	746197.26
436067.6	747399.98	456396.09	746987.89	448142.8	755181.66	440588.49	753580.01	435299.45	749321.22
437872.19	746910.69	438390.24	742320.59	446454.23	745980.87	441190.84	748911.76	432339.91	756429.17
438866.56	745995.24	440309.29	751133.98	448718.8	744471.15	447063.8	751547.06	434312.94	757365.09
436046.86	742894.39	438508.7	742273.21	450046.31	746319.25	438687.3	757947.08	437879.56	755822.08
436906.75	743472.72	455021.96	743291.96	452727.35	748089.26	435939.06	759678.85	435780.06	760919.07
434037.93	741151.79	440190.83	751133.98	453143.83	747022.05	436767.3	763801.21	440029.66	759856.67
437918.83	741920.36	439029.92	746206.06	449049.94	759377.43	442188.49	765100.04	442053.27	760919.07
431328.91	743876.03	437987.48	742344.28	453815.56	762167.67	453313.23	756798.84	439865.24	759995.79
437197.81	740579.96	437418.88	740543.7	449420.32	763105.98	447082.62	751584.71	432377.86	756403.87
434039.39	741136.43	440143.44	753076.71	454679.79	757451.43	453313.23	756817.66	442141.81	760994.95
440611.11	741893.81	450473.11	752792.41	456877.41	759895.97	447007.33	755970.6	437209.24	760969.66
441803.12	742705.58	434765.38	746750.97	455321.79	756537.81	454555.58	753580.01	434388.82	759907.26
446651.64	755620.79	443104.93	748883.25	457815.72	760291.05	455835.59	757965.9	435312.1	761741.16
444765.87	762710.49	446232.26	745590.07	457031.78	756771.23	443844.97	754502.36	439232.86	756884.48
455411.24	757604	440380.36	753763.78	450445.38	760637.16	445727.32	758191.78	441800.32	760021.09
440400.65	759107.12	449501.75	747532.81						
439782.93	761392.69	439219.46	753029.33						
434437.68	760504.99	450591.57	752887.18						
447036.31	757427.01	444028.92	760326.44						
436099.77	742586.66	443176.01	755327.44						
443541.79	741327.01	444028.92	760326.44						
447140.22	742366.86	439835.45	760113.21						
442392.48	737961.18	442417.87	762458.71						
446319.29	740205.07	454595.5	761037.19						
442674.28	737645.72	440119.75	755635.44						
446866.76	758339.08	445592.58	759899.98						
443880.22	759570.26	447961.77	751986.89						
445989.08	759277.7	452771.23	754972.07						
436775.25	760717.37	450378.35	752839.79						
442892.14	763160.34	451673.18	761010.47						
437362.32	764201.92	459123.08	760262.23						
433451.73	756598.48	438305.25	742390.29						
455641.19	756885.64	455864.53	745866.04						
443215.09	749628.38	438485.81	742345.15						
437132.57	749967.75	436273.97	748664.69						

Appendix 7. *Cumulative rainfall of all stations and each station (mm)*

Year	cum(all)	cum(Morocho)	cum(Ha/wita)	Cum(Aposto)	cum (Yirgalem)	cum (A/wondo)
1985	1311.77	1428.10	1329.70	928.39	1202.15	1670.51
1986	2870.91	3308.60	2751.30	2153.28	2634.57	3506.80
1987	4277.21	5166.60	3890.20	3412.41	3932.45	4984.40
1988	5822.36	7319.90	5144.39	4799.54	5362.26	6485.70
1989	7248.70	9163.80	6241.59	6296.45	6678.18	7863.50
1990	8556.20	10920.90	7203.49	7563.18	7881.11	9212.30
1991	9865.26	12486.30	8221.39	8936.08	9113.81	10568.70
1992	11253.08	14061.20	9564.99	10085.48	10404.81	12148.90
1993	12538.74	15351.20	10671.99	11194.68	11686.61	13789.20
1994	13848.58	16892.20	11738.69	12341.58	12920.61	15349.80
1995	15052.68	18929.70	12661.99	13403.48	14041.31	16773.90
1996	16576.60	21474.90	13830.39	14871.42	15513.51	18423.10
1997	17926.64	23360.94	14484.49	16230.92	16904.41	20389.09
1998	19248.42	24992.72	15749.79	17150.72	18559.01	21964.59
1999	20199.30	26287.53	16568.69	17825.72	19634.71	23202.19
2000	21268.88	27619.94	17572.49	18698.12	20706.41	24627.49
2001	22667.44	29295.05	18864.39	19626.92	22280.31	26600.29
2002	23664.36	30443.73	19725.17	20456.02	23277.51	28057.49
2003	24710.84	31836.15	20754.17	21305.22	24130.01	29540.59
2004	25734.10	33263.15	21782.07	22234.52	24962.81	30822.99
2005	27042.84	35026.43	23085.57	23265.92	26063.61	32641.09
2006	28534.76	36695.39	24543.77	24774.62	27486.51	34489.99
2007	30064.08	38476.99	26014.97	26151.62	28958.71	36512.89
2008	31192.44	39892.24	26945.17	27141.02	30182.81	37975.69
2009	32220.64	40937.03	27811.87	28154.92	31273.31	39381.29
2010	33533.98	42014.22	29172.57	29481.72	32501.51	41244.29
2011	34698.68	43490.11	30354.50	30812.62	33354.21	42622.59
2012	35751.65	44909.19	31253.68	31714.33	34561.81	43840.89
2013	36974.97	46402.06	32443.70	32959.33	35558.56	45433.61
2014	38327.10	47770.16	33832.40	34134.36	37016.78	47171.50
2015	39271.28	48745.64	34779.37	35151.41	37891.65	48339.88
2016	40545.11	50384.25	36187.17	36238.03	39233.81	49673.78